AD-A171 934 METAL OXIDE VARISTOR BURN-IN(U) AIR FORCE WEAPONS LAB 1/1
KIRTLAND AFB NM D H HILLAND JUN 86 AFWL-TR-85-151

UNCLASSIFIED F/G 9/1 NL

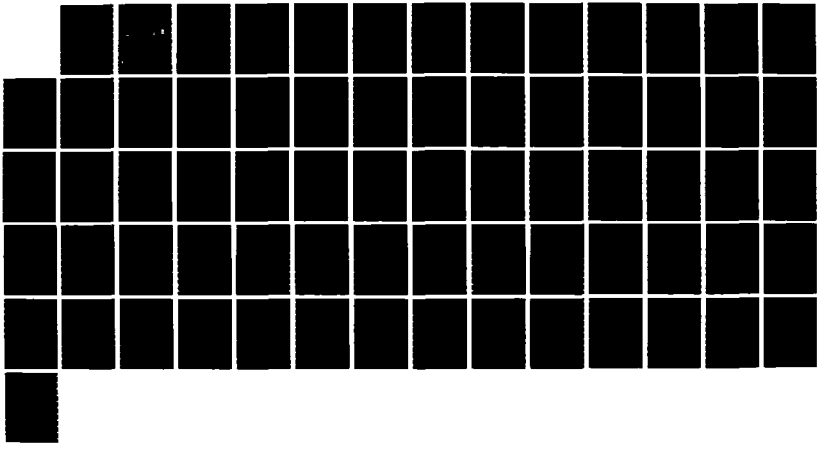

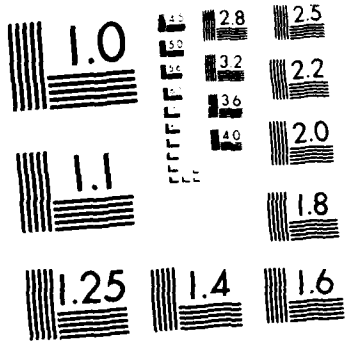
1.0
1.1
1.25
1.4
1.6
1.8
2.0
2.2
2.5
2.8
3.2
3.6
4.0

AFWL-TR-
85-151

(2)

AD-A171 934

METAL OXIDE VARISTOR BURN-IN

David H. Hilland

July 1986

DTIC
ELECTE
SEP 1 6 1986
D
D

Final Report

Approved for public release; distribution unlimited.

DTIC FILE COPY

AIR FORCE WEAPONS LABORATORY
Air Force Systems Command
Kirtland Air Force Base, NM 87117-6008

86 9 15 217

This final report was prepared by the Air Force Weapons Laboratory, Kirtland Air Force Base, New Mexico, under Job Order 88092603. Mr. David H. Hilland (NTAT) was the Laboratory Project Officer-in-Charge.

When Government drawings, specifications, or other data are used for any purpose other than in connection with a definitely Government-related procurement, the United States Government incurs no responsibility or any obligation whatsoever. The fact that the Government may have formulated or in any way supplied the said drawings, specifications, or other data, is not to be regarded by implication, or otherwise in any manner construed, as licensing the holder, or any other person or corporation; or as conveying any rights or permission to manufacture, use, or sell any patented invention that may in any way be related thereto.

This report has been authored by an employee of the United States Government. Accordingly, the United States Government retains a nonexclusive, royalty-free license to publish or reproduce the material contained herein, or allow others to do so, for the United States Government purposes.

This report has been reviewed by the Public Affairs Office and is releasable to the National Technical Information Service (NTIS). At NTIS, it will be available to the general public, including foreign nations.

If your address has changed, if you wish to be removed from our mailing list, or if your organization no longer employs the addressee, please notify AFWL/NTAT, Kirtland AFB, NM 87117 to help us maintain a current mailing list.

This technical report has been reviewed and is approved for publication.

David H. Hilland

DAVID H. HILLAND
Project Officer

FOR THE COMMANDER

Philip J. Messuri

PHILIP J. MESSURI
Major, USAF
Chief, Aircraft & Missile Division

Richard A. Paulsen

RICHARD A. PAULSEN
Captain, USAF
Chief, Technology Branch

DO NOT RETURN COPIES OF THIS REPORT UNLESS CONTRACTUAL OBLIGATIONS OR NOTICE ON A SPECIFIC DOCUMENT REQUIRES THAT IT BE RETURNED.

UNCLASSIFIED

SECURITY CLASSIFICATION OF THIS PAGE

AD A171 934

REPORT DOCUMENTATION PAGE

1a. REPORT SECURITY CLASSIFICATION: Unclassified	1b. RESTRICTIVE MARKINGS
2a. SECURITY CLASSIFICATION AUTHORITY	3. DISTRIBUTION/AVAILABILITY OF REPORT: Approved for public release; distribution unlimited.
2b. DECLASSIFICATION/DOWNGRADING SCHEDULE	
4. PERFORMING ORGANIZATION REPORT NUMBER(S): AFWL-TR-85-151	5. MONITORING ORGANIZATION REPORT NUMBER(S)
6a. NAME OF PERFORMING ORGANIZATION: Air Force Weapons Laboratory; 6b. OFFICE SYMBOL (If applicable): NTATI	7a. NAME OF MONITORING ORGANIZATION
6c. ADDRESS (City, State and ZIP Code): Kirtland Air Force Base, NM 87117	7b. ADDRESS (City, State and ZIP Code)
8a. NAME OF FUNDING/SPONSORING ORGANIZATION; 8b. OFFICE SYMBOL (If applicable)	9. PROCUREMENT INSTRUMENT IDENTIFICATION NUMBER
8c. ADDRESS (City, State and ZIP Code)	10. SOURCE OF FUNDING NOS.

PROGRAM ELEMENT NO.	PROJECT NO.	TASK NO.	WORK UNIT NO.
626210F	8809	26	03

11. TITLE (Include Security Classification): METAL OXIDE VARISTOR BURN-IN	
12. PERSONAL AUTHOR(S): Hilland, David H.	
13a. TYPE OF REPORT: Final Report	13b. TIME COVERED: FROM Aug 85 TO Nov 85
14. DATE OF REPORT (Yr., Mo., Day): 1986 June	15. PAGE COUNT: 70
16. SUPPLEMENTARY NOTATION	

17. COSATI CODES		
FIELD	GROUP	SUB. GR.
09	01	

18. SUBJECT TERMS (Continue on reverse if necessary and identify by block number): Varistor Degradation, Burn-In, Polarization

19. ABSTRACT (Continue on reverse if necessary and identify by block number)

Varistor degradation from unipolar transient pulsing is described. Metal-Oxide varistors (MOVs) subjected to a single high-energy transient displayed an increase in standby current and a decrease in clamping voltage. The amount of degradation was dependent on the polarity of the measurement relative to the polarity of the pulsing, as well as the energy rating of the device. After one pulse, the clamping voltage is lower when measured at the port opposite to the pulsing than when measured at the same port which was pulsed. Polarization of permanent electric dipoles in the insulating intergranular matrix and the filling of traps at the metal oxide grain boundaries are discussed as possible mechanisms for the degradation.

20. DISTRIBUTION/AVAILABILITY OF ABSTRACT: UNCLASSIFIED/UNLIMITED ☒ SAME AS RPT ☐ OTIC USERS ☐	21 ABSTRACT SECURITY CLASSIFICATION: Unclassified

22a. NAME OF RESPONSIBLE INDIVIDUAL	22b TELEPHONE NUMBER (Include Area Code)	22c. OFFICE SYMBOL
Mr. D. H. Hilland	(505) 844-9758	NTATI

DD FORM 1473, 83 APR EDITION OF 1 JAN 73 IS OBSOLETE

UNCLASSIFIED

SECURITY CLASSIFICATION OF THIS PAGE

CONTENTS

QUALITY INSPECTED 1

Accesion For	
NTIS CRA&I	☑
DTIC TAB	☐
Unannounced	☐
Justification	
By	
Distribution/	
Availability Codes	
Dist	Avail and/or Special
A-1	

INTRODUCTION

1. BACKGROUND

A varistor is a two-terminal, nonlinear terminal protection device used to clamp a circuit node at a specified value and shunt current away from the load being protected. In its nonconducting mode there is a small leakage current. In its conducting mode the voltage is clamped and large currents are shunted through the varistor to ground. The varistor has a response time of a few picoseconds so that the inductance in the leads is essentially the response time limiter. These devices are excellent for transient protection and applications have been expanding rapidly for the last 10 years. Several companies are manufacturing metal-oxide varistors (MOVs), including General Electric (GE) and Panasonic. These manufacturers have derating tables available for the user, but these data do not discuss the burn-in of low power varistors described in Ref. 1. Varistors with a clamping voltage of 18 V were found to have a 10 percent degradation in clamping voltage after the first transient was shunted and little degradation for subsequent transients. This was accompanied by an increase in the leakage current and general flattening of the I-V curve. Further burn-in phenomenon testing is described in Ref. 2 and is the subject of this report.

2. THEORY OF OPERATION

The exact physics of the nonlinear behavior of a zinc-oxide (ZnO) varistor is not known. Numerous explanations and models have been proposed. Most recently, holes have been added (Ref. 3) to the potential barrier model for the conduction process in the intergranular matrix. This addition has improved the amount of nonlinearity predicted by the model.

Figure 1 shows the grains and surrounding oxide matrix in a typical varistor. The nonlinear I-V curve is shown in Fig. 2 along with the standard power equation used to describe the curve. Alpha is used as a figure of merit and is typically between 20 and 50. Figure 2 shows that the varistor appears

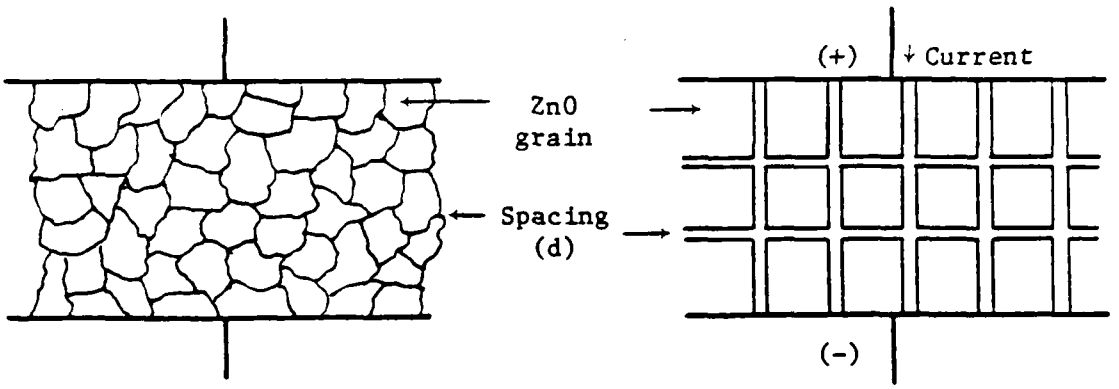

(a) Polycrystalline ZnO structure. (b) Idealized varistor.

Figure 1. Typical varistor composition.

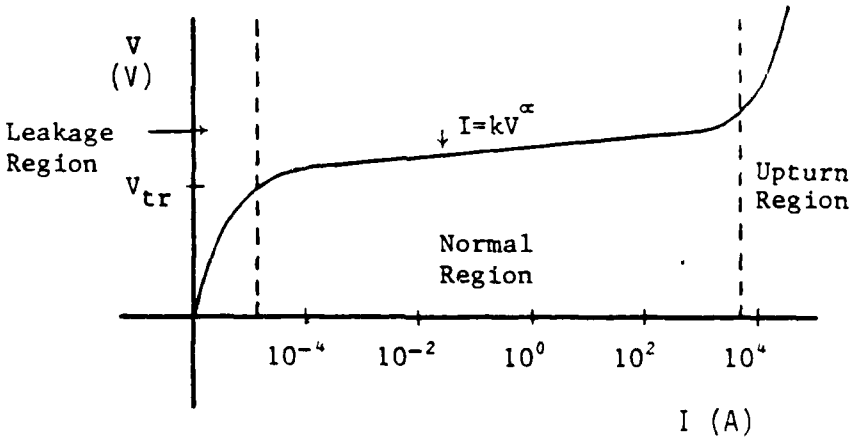

Figure 2. Typical I-V curve.

as an open circuit with a small leakage current in its nonconducting mode and as a small resistance in its conducting mode. The conducting mode is triggered by the threshold voltage appearing across the terminals.

Basically, electrostatic potential barriers are formed at the grain boundaries between the ZnO grains, which are equivalent to the depletion regions of p-n junction diodes. Conduction begins when the applied potential initiates tunneling of carriers between ZnO grains. The grains are relatively good conductors. The nonlinear characteristics of the device are provided by the combination of the grains with the bismuth and antimony oxide flux surrounding the grains. Experiments (Ref. 4) show that the dielectric constants for the ZnO and the intergranular matrix are approximately 10 and 16, respectively. The dielectric constant for the combination in a polycrystalline form is 1000. The resistivity of the oxide flux is much greater than the ZnO grains, so that the majority of an applied voltage is dropped across the regions between the ZnO grains. This is important for the discussion of polarization.

3. OBJECTIVE

The objective of this work is to determine if all five types of varistors manufactured by GE exhibit the same burn-in phenomenon seen in the low power V33MA1A tested in previous work (Ref. 1). This varistor had a significant degradation in the nominal clamping voltage with the first pulse applied, even when the pulse was within acceptable specifications for power and energy dissipation. The V33MA1A has been tested again along with the other four types.

TEST RESULTS

1. DISCUSSION OF EXPERIMENT

The experiment was conducted in the Direct Drive Laboratory of the Air Force Weapons Laboratory. A 100-J pulser was used for all devices. The pulser delivered a double exponential waveform with a 100-ns rise time and a 10-µs half pulse width. The test voltages are shown in Table 1. The test plan includes a more complete description of the pulser configuration and the required instrumentation.

2. DISCUSSION OF DATA

Five types of varistors were tested. The basic differences were in the clamping voltage specifications and the current handling capabilities. The package designs varied according to the current rating of the device. In general, the smaller devices tended to show more degradation than the larger devices. Polarization of the varistors was evident in all cases. Burn-in was evident in some cases.

The appendices include three sets of data: the varistor I-V curves for each varistor in Appendix A, the varistor voltage at two different currents as a function of the number of consecutive pulses in Appendix B, and data tables for those curves and the I-V curves data for varistor 21 in Appendix C.

Table 1. Varistor pulsing values.

V130HE150	RATED VOLTAGE (V)	RATED CURRENT (A)	TIME (µs)	INPUT XFRM-V (kV)	PULSER CHARGE-V (kV)
V33MA1A	150	40 A	10	3.3	9.9 (3X)
V47ZA7	200	1000 A	10	4.4	13.2 (3X)
V275LA40A	1.3	10 A	10	28.6	28.6
V250PA40C	1.1	5 A	10	24.2	24.2
V130HE150	550	10 A	10	12.1	12.1

The varistor I-V curves show that some polarization was achieved in all five types of varistors by using a unipolar pulse. The degradation was frequently greater in one direction through the varistor than in the other, indicating polarization of the intergranular matrix. The varistor V-pulse curves in Appendix B show that the polarization occurs in the direction opposite to the pulsing. In other words, the voltage at 1 mA is lower in the negative direction than in the positive direction after pulsing in the positive direction. This was consistent for all the devices. In all cases the pulse energy was below the maximum level allowed by the specifications.

The data tables show the raw numbers used to generate the V-pulse curves. Some devices were tested for more cumulative pulses than others. The decision to continue pulsing was based on the amount of degradation apparent from the raw data and on the survival rate for the type of device under test. The raw data for the I-V curves are not included with this report. The plots serve to illustrate the qualitative parameters under study.

2.1 V33MA1A--This varistor has a nominal voltage of 33 V at 1 mA and a 200-mW power rating. The I-V curves for varistors 2 through 5, Figs. A-2 through A-5, show a definite difference in the amount of degradation in the early part of the curve based on the polarity of the curve data. The difference is less noticeable for device 1. Figures B-2 through B-5 show this more clearly. The degradation is more pronounced for the 0.1 mA data than for the 1 mA data. It is evident by an increase in the leakage current and a reduction in the switch-like nonlinear behavior of the device. As the varistor degrades, it acts more like a resistor as can be seen in Figs. A-1 through A-5. These results are consistent with those of the first experiment.

2.2 V47ZA7--This varistor has a nominal voltage of 47 V at 1 mA and a power rating of 600 mW. Figures A-6 through A-10 show a consistent burn-in and less consistent degradation with additional pulsing. The polarization is particularly evident in varistors 21, 23, and 24, where the flattening of the curve is greatest measured in the polarity opposite to the pulsed polarity. Figures B-6 through B-10 show that the polarization is even greater for the

V47ZA7 than for the V33MA1A. For varistor 21, there is a 10-V difference in clamping voltages at both 0.1 mA and 1 mA after 1 and 2 consecutive pulses, depending on the polarity of the measurement.

2.3 V275LA40A--This varistor has a nominal voltage of 430 V at 1 mA and a transient power rating of 1 W. Figures A-11 through A-14 are less consistent with the results needed to support the burn-in explanation. This could be due to the increased current rating of these devices. Varistor 31 looks like the previous plots but varistors 32 and 33 are not sufficiently separated to allow for the error associated with these measurements. Figure B-12 shows polarization for varistor 31. Figure B-13 shows that an error was made in recording the data resulting in an improper curve fit. Figure B-14 shows polarization for varistor 33 but the data points at eight consecutive pulses and 0.1 mA appear to be high by 100 V.

2.4 V250PA40C--This varistor has a nominal voltage of 390 V at 1 mA and a transient power rating of 1.5 W. The PA series of varistors are not as strong as the LA series. These PA type devices exhibit both polarization and burn-in for the measured polarity, which is opposite to the pulsed polarity in every case. However, the burn-in was small or not evident in the like polarities for varistors 41, 43, and 44. In general, more pulses were required and consequently more cumulative energy was required to degrade the type LA and PA varistors than the smaller type MA and ZA varistors. Figure A-17 shows degradation for consecutive pulsing similar to the smaller varistors. Figures B-16 through B-19 show significant polarization for all four varistors. The starting data point for the 1 mA negative polarity measurement in Figure B-16 appears to be in error.

2.5 V130HE150--This varistor has a nominal voltage of 200 V and a transient power rating of 1.5 W. This varistor is rated at 20 kA for 20 μs which is considerably more than the other varistor current ratings. The type HE varistors have the highest energy rating of the five types tested. The test results are consistent with this high energy rating. The drop in the I-V curve was consistent for the measured polarity opposite to the pulsed polarity. Varistors 51 and 52 did not degrade for the common polarity case after 13 cumulative shots.

2.6 Standard Deviation and Error Bars--No error bars are included with these curves because the plotting routine did not support this feature. The standard deviation for the DC I-V data was calculated to be within 1 V. The method for this determination was discussed in Ref. 1.

3. DEGRADATION

There are two mechanisms which are likely candidates for the burn-in phenomenon recorded by this experiment. One is the filling of traps in the intergranular matrix. The other is the polarization of permanent electric dipoles which exist in the structure of the intergranular matrix.

The integranular material in a varistor is an insulator. The primary ingredients are bismuth and antimony oxides with much smaller amounts of cobalt, manganese and chromium oxides. The ZnO grains are good conductors relative to the surrounding matrix. A space charge region is formed at all interfaces between the two materials. Figure 3 shows the space charge region with traps in the insulator. The space charge region's characteristics will be affected by changes in the density of traps. The relationship between the trap density and the varistor characteristics; $V_{n(DC)}$ (the nominal clamping voltage), and alpha (the figure of merit for the varistor from the slope of the I-V curve) is developed from basic insulator solid state physics.

For low voltages, the insulator follows Ohm's law.

$$J = en_0\mu\frac{V}{L} \qquad (1)$$

where

J = the current density, A/cm^2
e = the electron charge in Coulombs
n_0 = the thermal carrier density, electrons/cm^2
μ = the free carrier mobility (very small for an insulator)
V = the applied voltage
L = the thickness of the insulator, cm

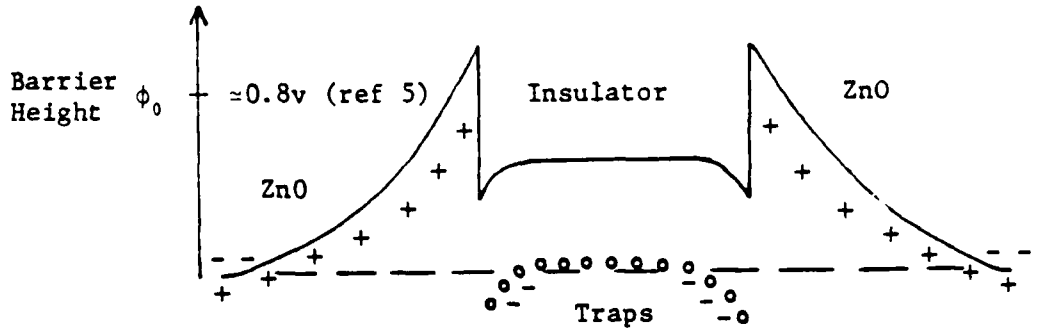

(a) No voltage applied.

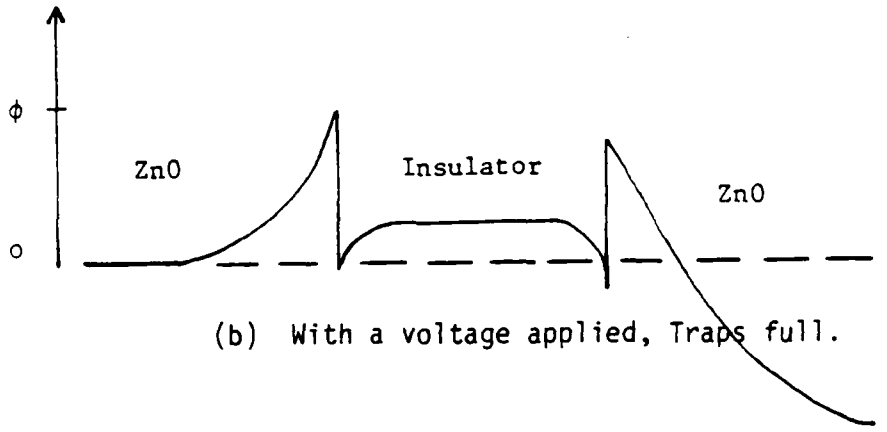

(b) With a voltage applied, Traps full.

Figure 3. Potentials at the interface.

At the transition between ohmic and nonlinear behavior, the Mott-Gurney law (Ref. 10) is used. This transition occurs at some threshold voltage, V_{tr}, determined by,

$$en_0L = Q_{injected} = CV_{tr} = \frac{\epsilon}{LV_{tr}} \tag{2}$$

$$V_{tr} = \frac{en_0L^2}{\epsilon} \tag{3}$$

where

ϵ = the permittivity of the insulator, F/m

In order for nonlinear conduction to occur, the injected excess free electron density, n, becomes approximately equal to the thermally generated electron density, n_0, (Ref. 4); i.e.,

$$n \approx n_0$$

Between the conduction and valance bands, the free electron density

$$n_o = N_c \exp\left(\frac{F_{td} - E_d}{kT}\right) \tag{4}$$

where

N_c = the effective density of states in the conduction band
F_{td} = the thermodynamic Fermi level
E_c = the energy level for the bottom of the conduction band
kT = the thermal energy

from Fermi-Dirac, the electron trap occupancy is

$$n_t = \frac{N_t}{1 + \frac{1}{g} \exp\left(\frac{E_t - F_{td}}{kT}\right)} \tag{5}$$

where

N_t = the trap density
E_t = the trap energy level
g = the trap generation factor

The thermal equilibrium exists when the electron generation equals the electron capture rate. This balance is not significantly affected by the application of a small electric field. The equilibrium is calculated with the free electron density which includes the injected electrons, $n(x)$ from a small electric field.

$$n(x) = N_c \exp\left(\frac{F_n(x) - E_c}{kT}\right) \tag{6}$$

where

$F_n(x)$ = the electron steady state Fermi level.

Now the electron trap occupancy with the injected electrons is:

$$n_t(x) = \frac{N_t}{1 + \frac{1}{g}\exp\left(\frac{E_t - F_n(x)}{kT}\right)} \tag{7}$$

and a thermal equilibrium with some free carriers exists.

It is convenient to simplify Eq. 7 further to illustrate the relationship between the traps and the carriers.

Let

$$N = N_c \exp\left(\frac{E_t - E_c}{kT}\right) \tag{8}$$

then

$$\frac{N}{n(x)} = \frac{N_c \exp\left(\frac{E_t - E_c}{kT}\right)}{N_c \exp\left(\frac{F_n(x) - E_c}{kT}\right)}$$

$$\frac{N}{n(x)} = \exp\left(\frac{E_t - E_c}{kT}\right) \exp\left(\frac{E_c - F_n(x)}{kT}\right)$$

$$\frac{N}{n(x)} = \exp\left(\frac{E_t - F_n(x)}{kT}\right) \tag{9}$$

and

$$n_t(x) = \left(\frac{N_t}{1 + \frac{N}{gn(x)}}\right) \tag{10}$$

The denominator of Eq. 10 represents the effect of the relative energy level of the traps. There are two cases of interest which simplify this denominator further.

As long as $E_t - F_n(x) > kT$ then

$$1 + \frac{N}{gn(x)} \approx \frac{N}{gn(x)} \tag{11}$$

and the traps are labeled "shallow". For shallow traps the ratio of free electron density to trapped electron density is a constant independent of n(x), the free carrier density at position x. In other words, from Eqs. 10 and 11,

$$\frac{n(x)}{n_t(x)} = \frac{N}{gN_t} = C \tag{12}$$

When traps are considered in Eqs. 1 and 3 for J and V_{tr}, this constant, C, reduces the transition voltage between the ohmic and nonlinear conduction regions of the insulator.

$$J = Cen_0\mu L^2 \tag{13}$$

and

$$V_{tr} = \frac{en_0L^2}{C\epsilon} \tag{14}$$

For the case when $F_n(x) > E_t$, the exponential power in Eq. 7 is negative and

$$n_t(x) \approx N_t \tag{15}$$

The traps in this case are labeled "deep". The electron injection level determines the relative differences between shallow and deep traps. As n(x) increases, $F_n(x)$ moves higher toward the conduction band through the forbidden energy gap.

As $F_n(x)$ moves through a shallow trap at E_t, that trap becomes a deep trap. This alters the I-V characteristics of the insulator.

As a general rule, current injection becomes dominant when the voltage applied is sufficient to double the free carrier density, $n = 2n_0$.

At this density, all of the traps are full below E_t and,

$$V_{tr} = \frac{eN_t L^2}{\epsilon} = V_{TFL} \tag{16}$$

where

V_{TFL} = the voltage with the traps filled to the limit below E_t

Armed with an expression for a threshold voltage as a function of the density of traps, consider the probable mechanisms by which burn-in could occur. Burn-in was evident from a reduced voltage in the nonlinear region of the curve and by a reduced α. The reduced α is evident in both directions for the smaller varistors and in the direction opposite to pulsing for the larger varistors.

Using Eq. 16, if N_t, the density of traps is reduced then the voltage is reduced. If ϵ, the permittivity is increased, the voltage is reduced.

Also when $n = 2n_0$, the ratio of currents at $2V_{TFL}$ is,

$$\frac{I(2V_{TFL})}{I(V_{TFL})} \approx \frac{2n(2V_{TFL})}{n(V_{TFL})} \approx \frac{N_t}{n_0} \tag{17}$$

This approximation can be used in the equation for α.

$$\alpha = \frac{\log\left(\frac{I_2}{I_1}\right)}{\log\left(\frac{V_2}{V_1}\right)} = \frac{\log\left[\frac{I\left(2V_{TFL}\right)}{I\left(V_{TFL}\right)}\right]}{\log 2} \tag{18}$$

$$\alpha \approx 3.32 \log\left(\frac{N_t}{n_0}\right) \tag{19}$$

So, if N_t is reduced, α is also reduced.

Evidence suggests that both N_t is reduced and α is increased. This would account for a burn-in degradation in either polarity and a greater degradation in the polarity opposite to the pulsed polarity. The density of traps may be reduced simply by filling deep traps which remain filled after the initial pulse. This would be more pronounced with smaller, thinner varistors that have fewer interfaces between the grains. This could occur in conjunction with the mechanism for raising the permittivity, which is polarization.

The insulating matrix consists of molecules which are more loosely bound than those in the ZnO grains. The flux surrounding the grains is sintered at 1350°C so that all grains are coated but none of the key ingredients are evaporated. Permanent electric dipoles exist in the intragranular matrix. A molecule will have a permanent electric dipole moment if the centers of positive and negative charge do not coincide. This occurs with all five of the typical ingredients in MOV insulators. Cobalt oxide and manganese oxide are diatomic heteronuclear molecules whose charge centers do not coincide. The dipole moment is given by,

$$p = (q) \times (r) \tag{20}$$

where

q = the amount of charge
r = the separation between the charge centers.

The separation, r, is usually taken as the measured bond length from x-ray diffraction. The charge, q, can be calculated from the measured dipole moment..

Polyatomic molecules such as bismuth, chromium and antimony oxides also have permanent dipole moments. Reorientation as a result of high voltage pulsing would reduce the electric field sustainable across the varistor. Recall that the ZnO grains are good conductors relative to the other material. A change in the electric field in the intergranular matrix could significantly

affect the varistors as a whole. The intergranular bonds are weak enough to allow polarization but strong enough to prevent the dipoles from relaxing immediately when the electric field is removed.

Recall the polarization vector,

$$P = X_e \epsilon_0 E = D - \epsilon_0 E \tag{21}$$

$$X_e = \frac{\epsilon}{\epsilon_0 - 1} \tag{22}$$

$$D = \frac{q}{A} \tag{23}$$

where

ϵ = the permittivity $\epsilon_r \epsilon_0$
ϵ_r = the relative permittivity or dielectric constant
ϵ_0 = the permittivity of free space, $\approx 8.85 \times 10^{-12}$ F/m
E = the electric field strength
D = the electric flux density
A = the area over which the field is distributed
d = the thickness of the material

The voltage across the device can be found from

$$V = Ed \tag{24}$$

$$\frac{P}{\epsilon_0} = \frac{q}{\epsilon_0 A} - E \tag{25}$$

$$\frac{Pd}{\epsilon_0} = \frac{qd}{\epsilon_0} - V$$

$$V = V_{applied} - \frac{Pd}{\epsilon_0} \tag{26}$$

So, the polarization adds to or subtracts from the applied voltage, depending on its sign. In this case, ϵ is very large ($\approx 1000\epsilon_0$), therefore, P is very large.

As example, consider varistor 21, type V47ZA7. Equation 18 will serve to calculate the α's which can be used to show the change in N_t and the polarization. Using Eq. 18,

$$\alpha_{0+} = \frac{1}{\log\left(\frac{47.43}{43.45}\right)} = 26.27$$

$$\alpha_{0-} = \frac{1}{\log\left(\frac{47.68}{43.26}\right)} = 23.67$$

$$\alpha_{1+} = \frac{1}{\log\left(\frac{44.90}{36.00}\right)} = 10.42$$

$$\alpha_{1-} = \frac{1}{\log\left(\frac{38.09}{25.41}\right)} = 5.17$$

where + and - indicate the polarity of the measurement. If the polarization is removed, numerically, by

$$38.09 + \left(44.90 - \frac{38.00}{2}\right)$$

then

$$\alpha_0 = \frac{1}{\log\left(\frac{47.43 + \left(\frac{47.68 - 47.43}{2}\right)}{43.26 + \left(\frac{43.45 - 43.26}{2}\right)}\right)} = 24.9$$

$$\alpha_1 = \frac{1}{\log\left(\frac{38.09 + \left(\frac{44.90 - 38.09}{2}\right)}{25.41 + \left(\frac{36.00 - 25.41}{2}\right)}\right)} = 7.6$$

Now these α's can be substituted in Eq. 19. Let $\rho_L = 10^{13}$ Ω cm and $\mu = 1$ cm^2/Vs. If

$$n_0 = \frac{1}{\rho_L e \mu} \approx 10^5/cm^3 \tag{27}$$

Then from Eq. 19, $N_{t\alpha 0} = 3.2 \times 10^{12}$ and $N_{t\alpha 1} = 2.0 \times 10^7$, so N_t was reduced from 10^{12} to 10^7 by the filling of traps with the first pulse.

Now if the polarization is calculated for the change from zero pulses to one pulse on varistor 21, from Eq. 26,

$$\Delta V_{2,1} = 44.90 - 38.09 = 6.81$$

$$\Delta V_{1,1} = 36.00 - 25.41 = 10.59$$

$$\frac{\Delta V_{2,1}}{2} = 3.4 \text{ V} = \frac{P_2 d}{\epsilon}$$

$$\frac{\Delta V_{1,1}}{2} = 5.3 \text{ V} = \frac{P_1 d}{\epsilon} \tag{28}$$

where $\Delta V_{2,1}$ is the voltage difference between the positive and negative polarity measurements at 1 mA after 1 puse. The $\Delta V_{1,1}$ is the voltage difference between the positive and negative polarity measurements at 0.1 mA after 1 pulse. The raw data for varistor 21 are included in Appendix C. The raw data for the entire experiment are available but not included here. The thickness, d, of the varistor is proprietary. However, the polarization left in the form shown serves to illustrate the + or - effect on the applied voltage.

It has shown that the α's and the clamping voltages are reduced by pulsing and that a change in the filled trap density along with a change in the polarization may be responsible. Further work could be done to measure the actual trap densities and the polarization before and after pulsing. This may be difficult to do nondestructively.

CONCLUSIONS

Varistors are subject to degradation. The burn-in and subsequent degradation seen in the data can be explained by the filling of traps at the grain boundaries and the polarization of the permanent electric dipoles in the intergranular matrix. A reduction in the density of filled traps from 1×10^{12} to 1×10^{7} appears excessive. However, the value for the thermal carrier density taken from Ref. 5 may also be low. Further work is needed to quantify the trap density experimentally before and after the burn-in.

The evidence presented suggests that the varistor material polarizes as a result of unipolar pulsing and that the clamping voltage and leakage current are degraded. The new low power line of varistors are more susceptible to this degradation than larger models. Smaller varistors are thinner and have less grain boundaries, so degradation as a result of both traps and polarization is more pronounced. This conclusion is well supported by the fact that the degradation occurs for all five sizes of varistors when the measured polarity is opposite to the pulsed polarity. But when the measured polarity is in the same direction as the pulsed polarity, only the smaller devices with lower power ratings exhibit degradation.

The popularity of varistors as overvoltage protection is increasing and the user must be aware of the conditions which degrade varistors and the amount of degradation to expect for a given varistor in a given application. Care should be taken in the selection of a varistor to allow for degradation. In some cases a monitoring system may be required to detect degradation below some threshold. The testing done in this study concerns unipolar pulsing of varistors below the rated energy level in joules. A comprehensive study of the sources of both bipolar and unipolar transients would also be helpful.

REFERENCES

1. Hilland, D. H., Metal Oxide Varistor Degradation, AFWL-TR-85-117, Air Force Weapons Laboratory, Kirtland Air Force Base, New Mexico, September 1985.

2. Hilland, D. H., Test Plan for Varistor Burn-In Experiment, AFWL-TN-85-53, Air Force Weapons Laboratory, Kirtland Air Force Base, New Mexico, October 1985.

3. Pike, G. E., Kurtz, S. R., Gourley, P. L., Phillip, H. R., and Levinson, L. M., "Electroluminescence in ZnO Varistors: Evidence for Hole Contributions to the Breakdown Mechanism," Journal of Applied Physics, Vol. 57, No. 12, 14 June 1985.

4. Matsuoka, Michio, "Nonohmic Properties of Zinc Oxide Ceramics," Japanese Journal of Applied Physics, Vol. 10, No. 6, June 1971.

5. Lampert, Murray A., "Injection Current in Insulators," Proceedings of the IRE, No. 50, pp 1781-1796, 1962.

6. Beam, W. R., Electronics of Solids, McGraw-Hill Book Co., pp 345-359, 1965.

7. Harnden, J. D. Jr., Martzloff, F. D., Morris, W. G., and Golden, F. G., "Metal-Oxide Varistor: A New Way to Suppress Transients," Electronics Magazine, 9 October 1972.

8. Levinson, Lionel M. and Phillip, Herbert R., "ZnO Varistors for Transient Protection," IEEE Transactions of Parts, Hybrids and Packaging, Vol. PHP-13, No. 4, pp 338-343, December 1977.

9. Emtage, P. R., "The Physics of Zinc Oxide Varistors," Journal of Applied Physics, Vol. 46, No. 10, pp 4372-4384, October 1977.

10. Kittel, Charles, "Introduction to Solid State Physics," John Wiley and Sons, Inc., Fifth edition, pp 400-415, 1976.

11. Bowen, L. J. and Avella, F. J., "Microstructure, Electrical Properties, and Failure Prediction in Low Clamping Voltage Zinc Oxide Varistors," Journal of Applied Physics, Vol. 54, No. 5, May 1983.

12. Golden, F., et al., Transient Voltage Suppression Manual, Fourth edition, General Electric Company, Auburn, New York, 1983.

APPENDIX A

VARISTOR I-V CURVES

Appendix A contains the varistor I-V curves for all varistors tested. The curves are labeled with the varistor number, the pulsed polarity and the measured polarity. The legend identifies the progressive degradation in the I-V characteristics with successive pulsing.

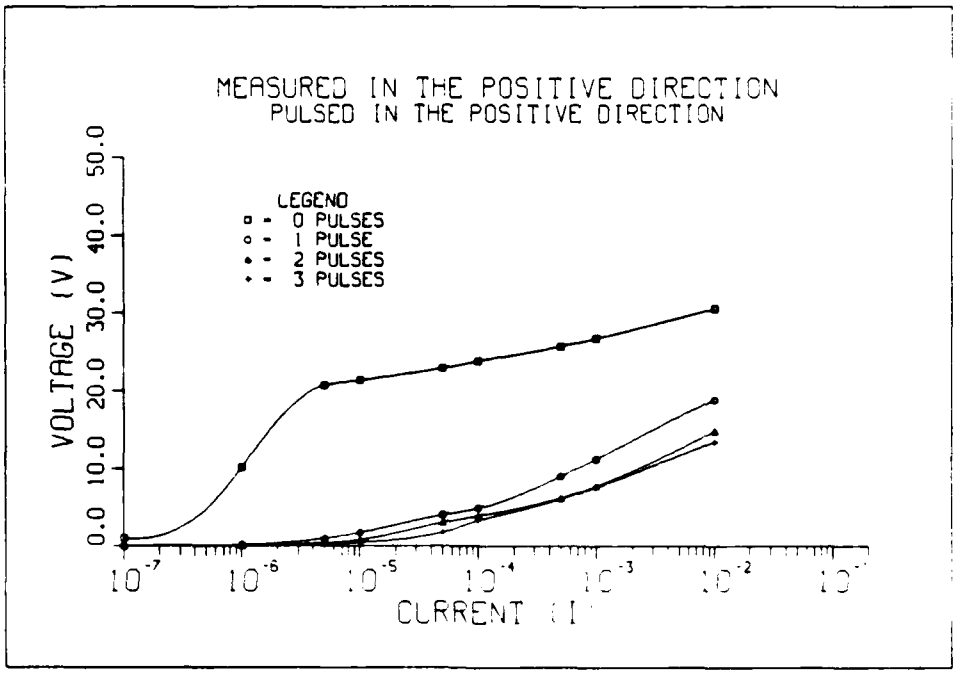

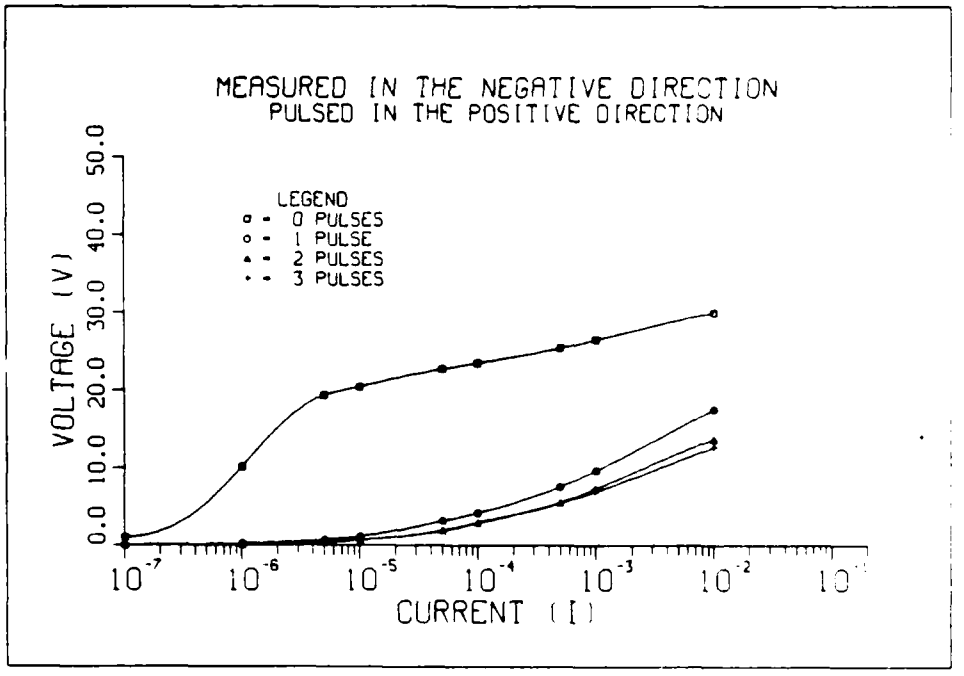

Figure A-1. I-V curves for varistor 1.

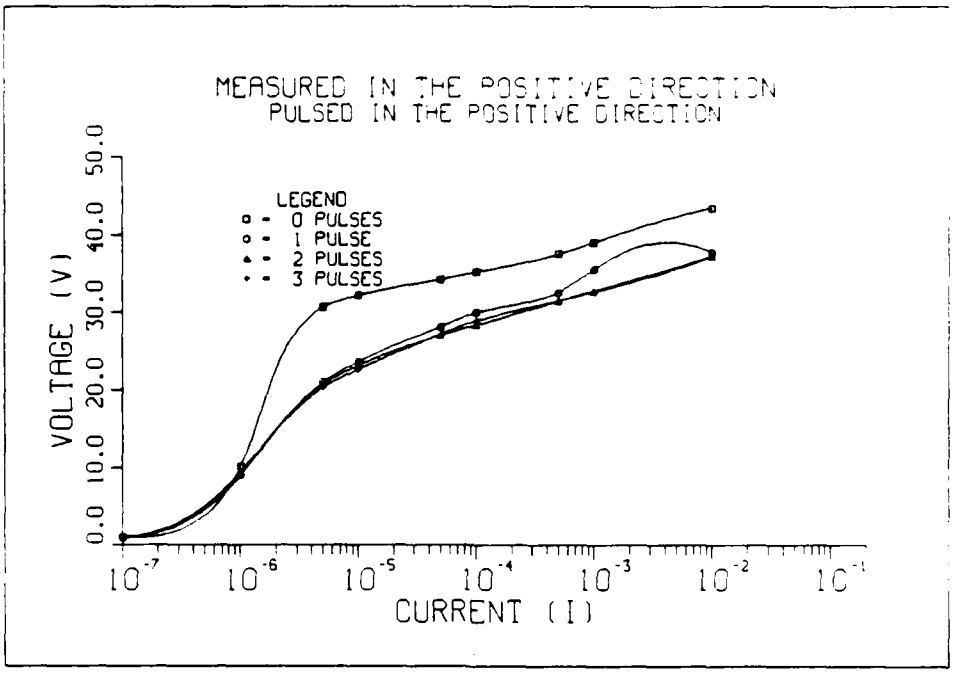

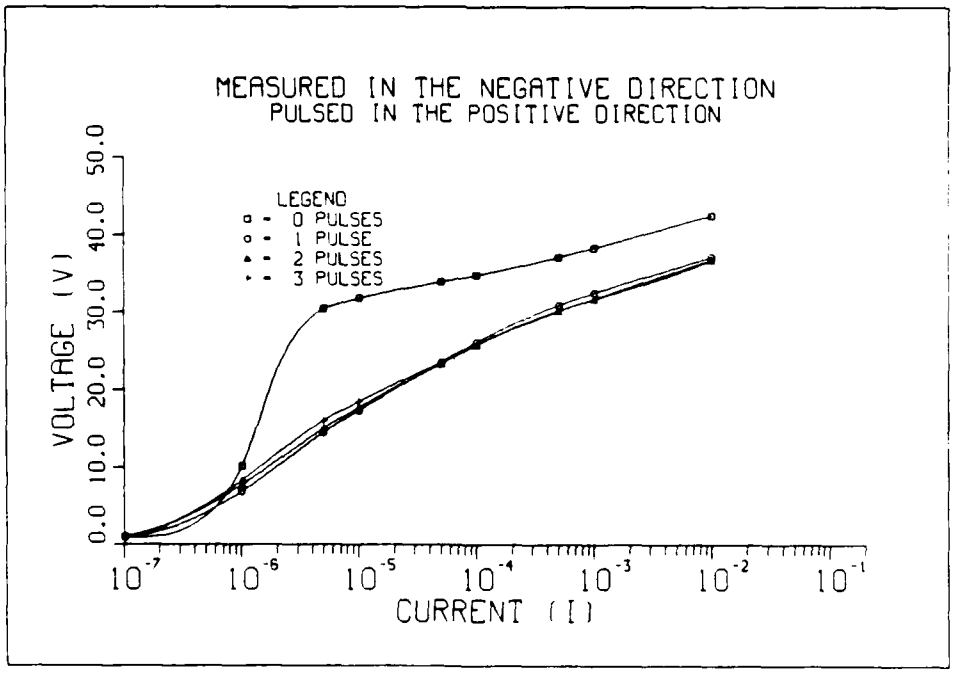

Figure A-2. I-V curves for varistor 2.

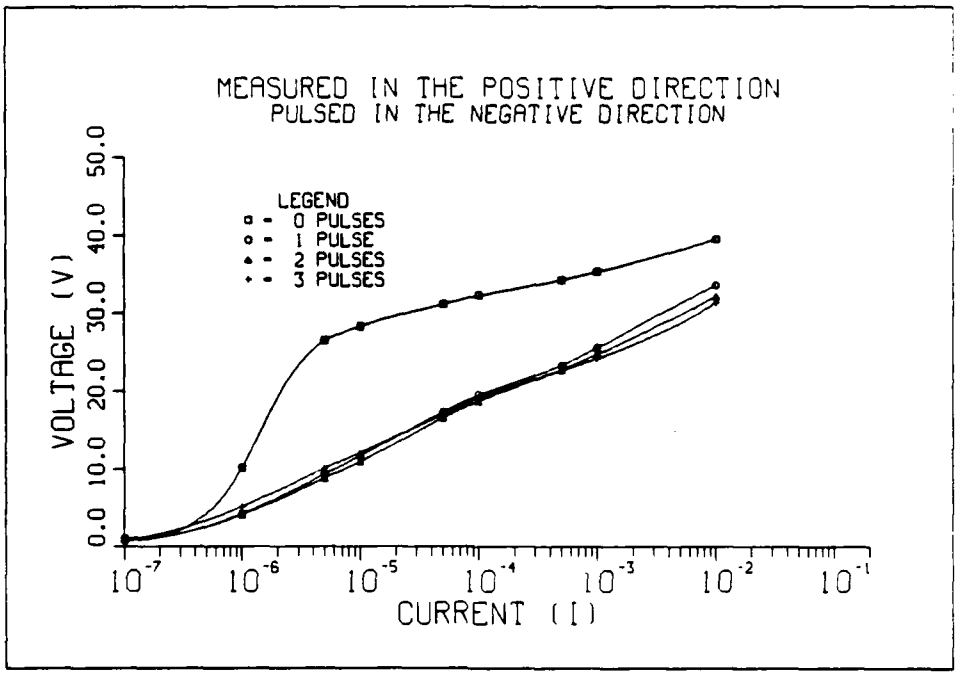

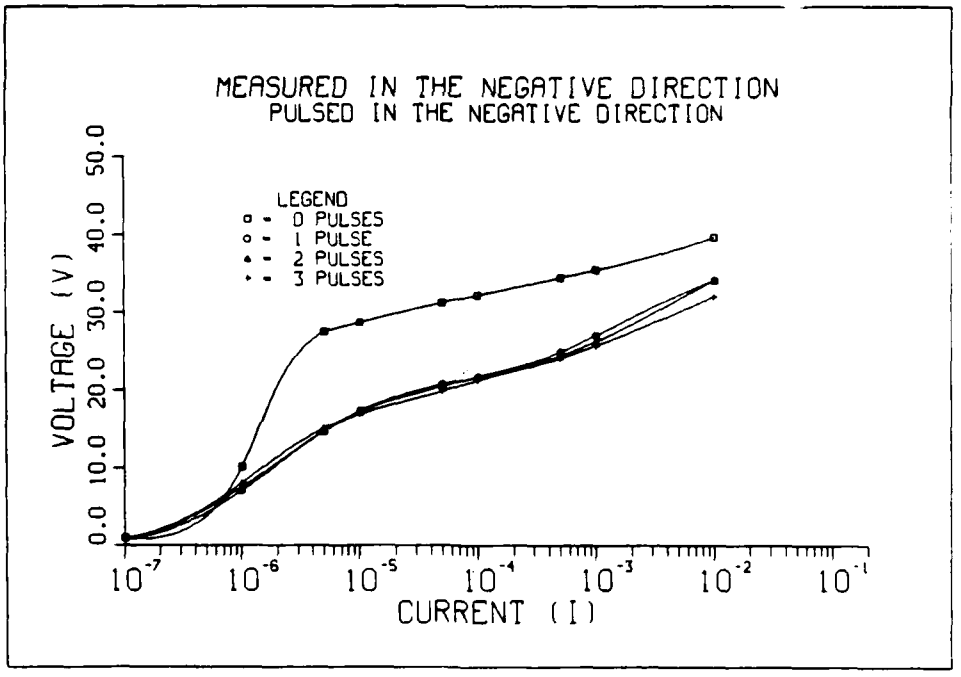

Figure A-3. I-V curves for varistor 3.

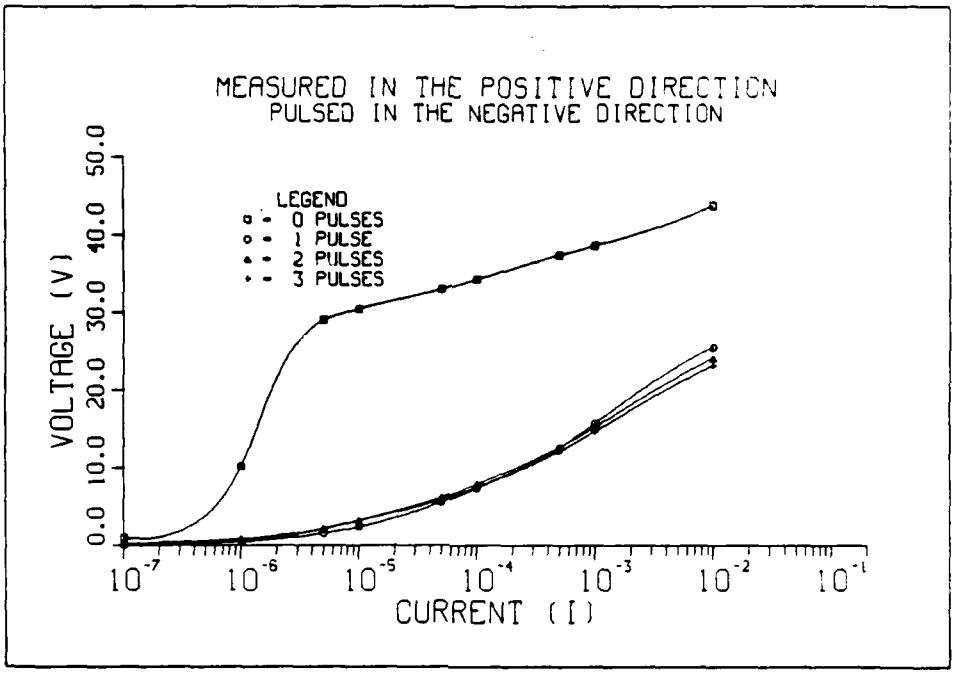

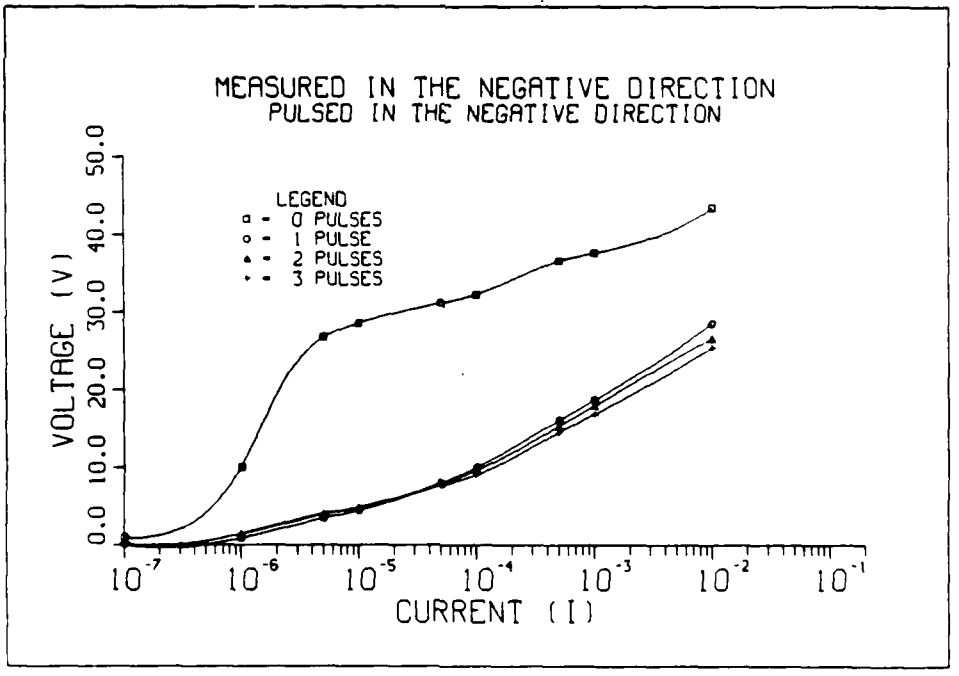

Figure A-4. I-V curves for varistor 4.

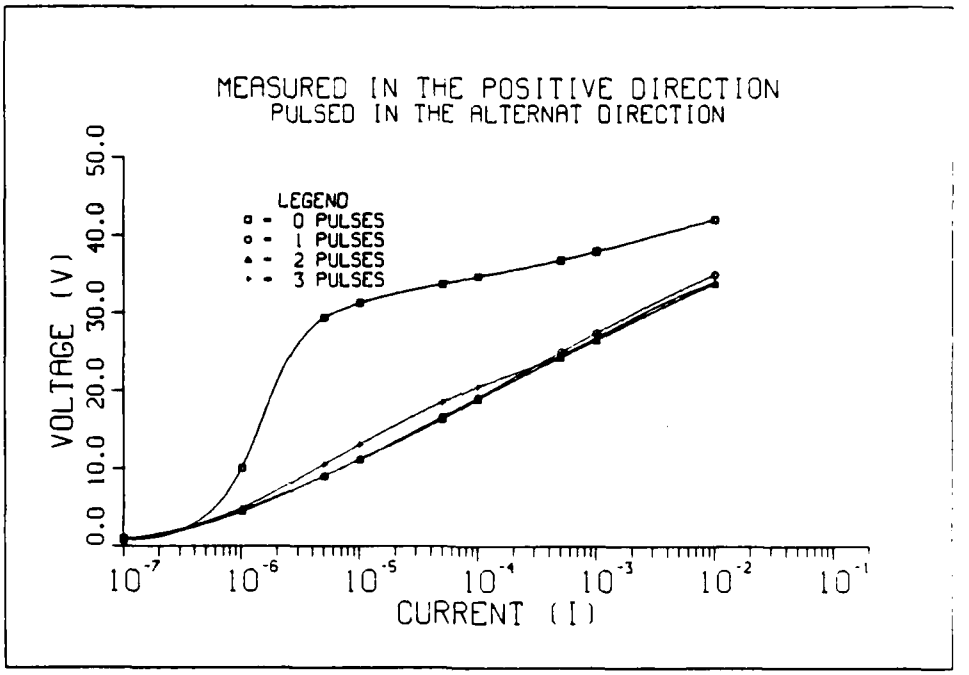

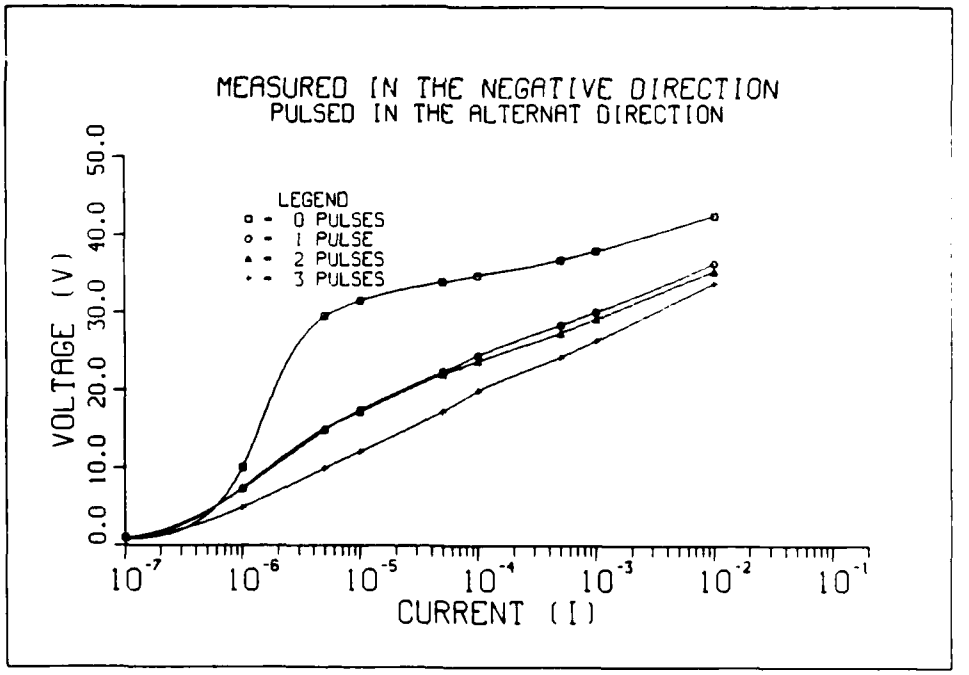

Figure A-5. I-V curves for varistor 5.

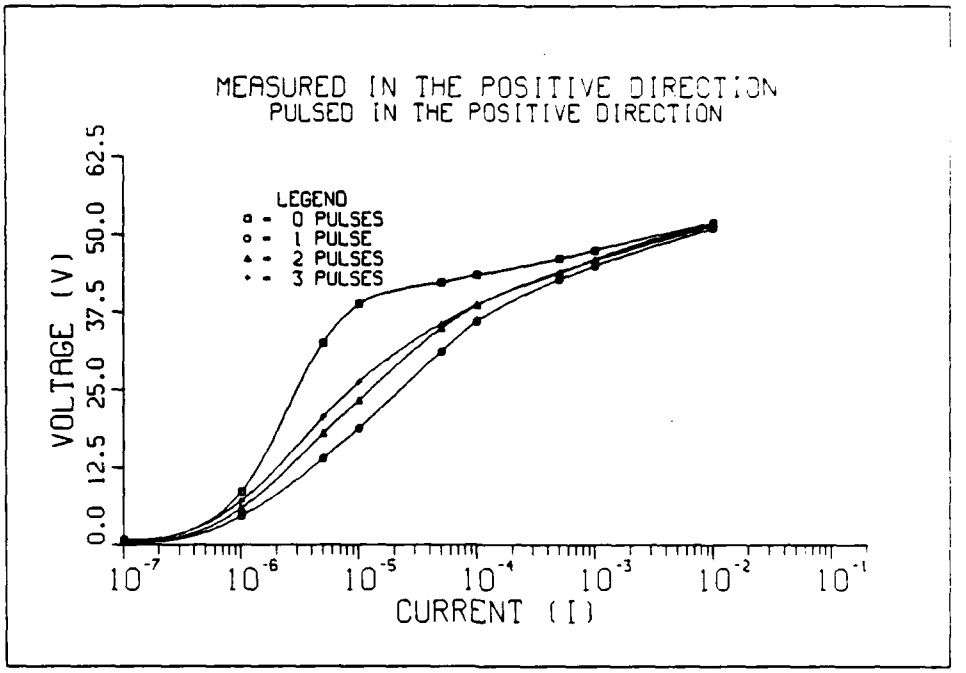

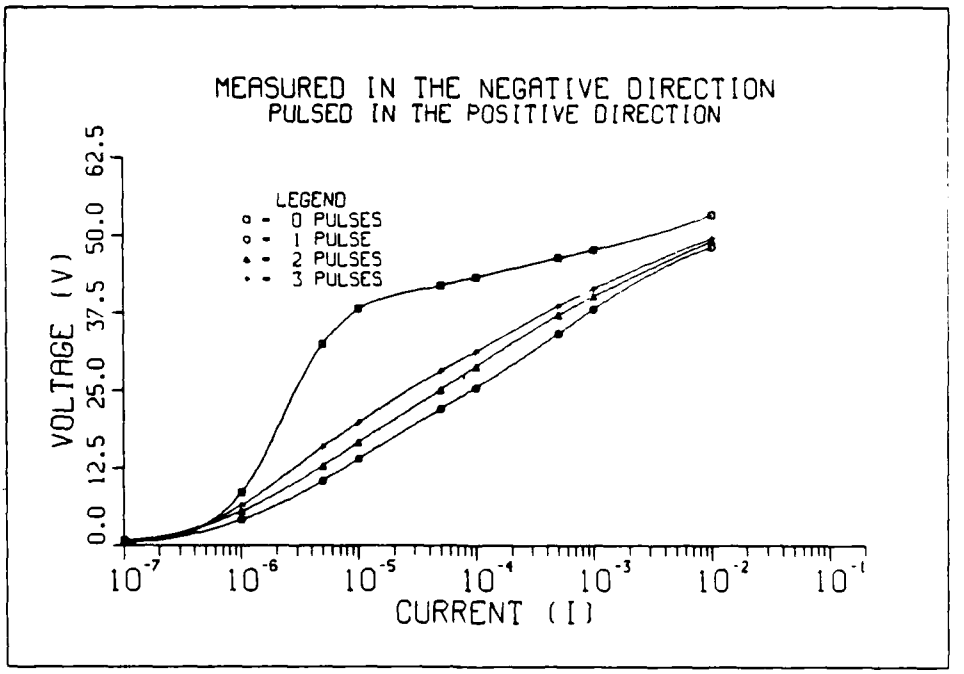

Figure A-6. I-V curves for varistor 21.

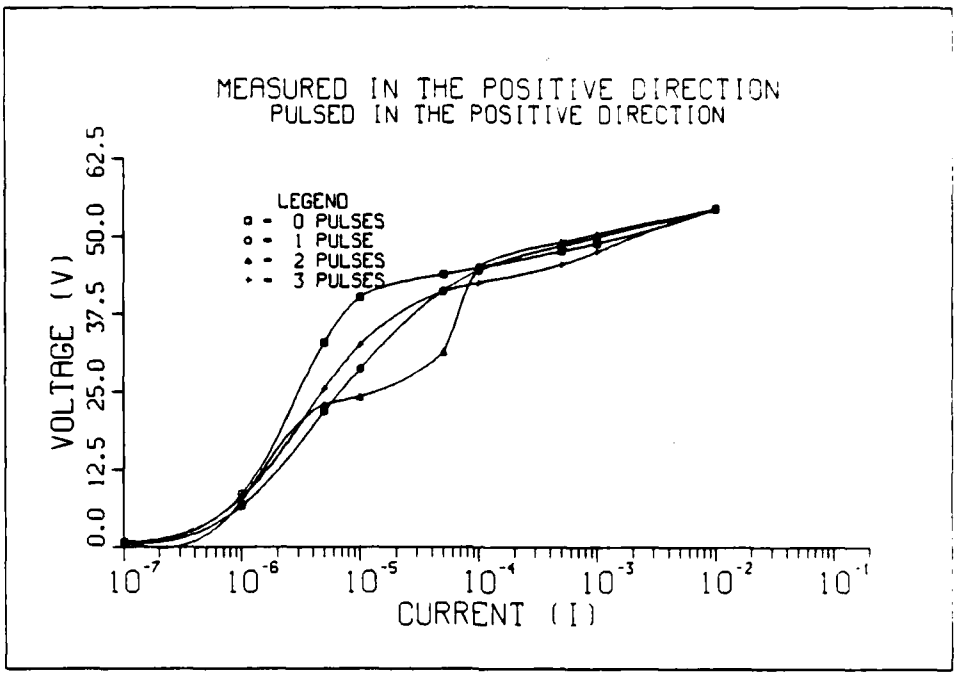

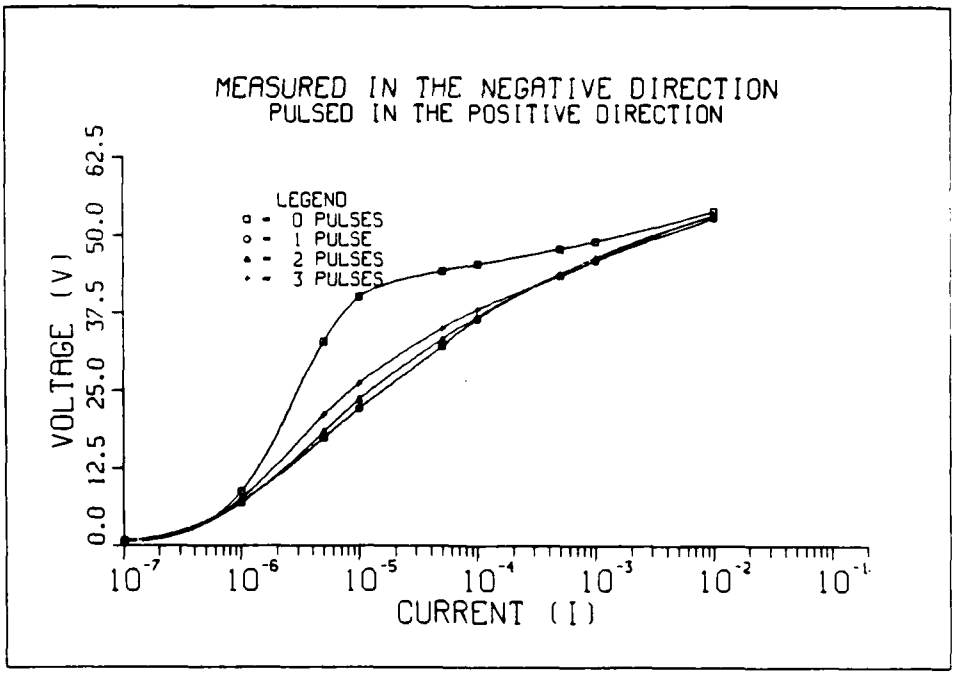

Figure A-7. I-V curves for varistor 22.

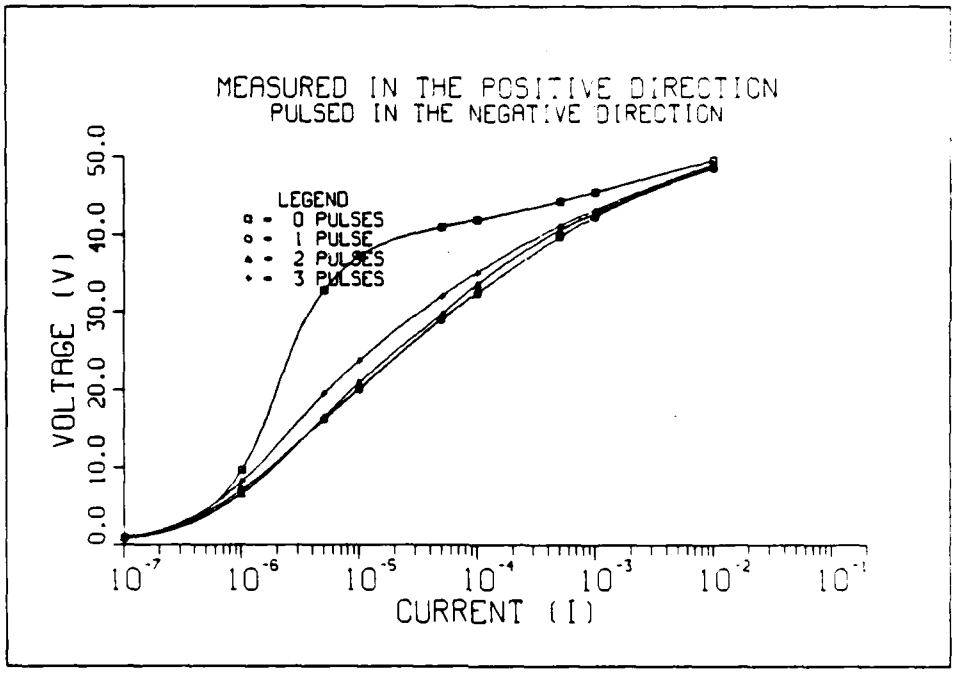

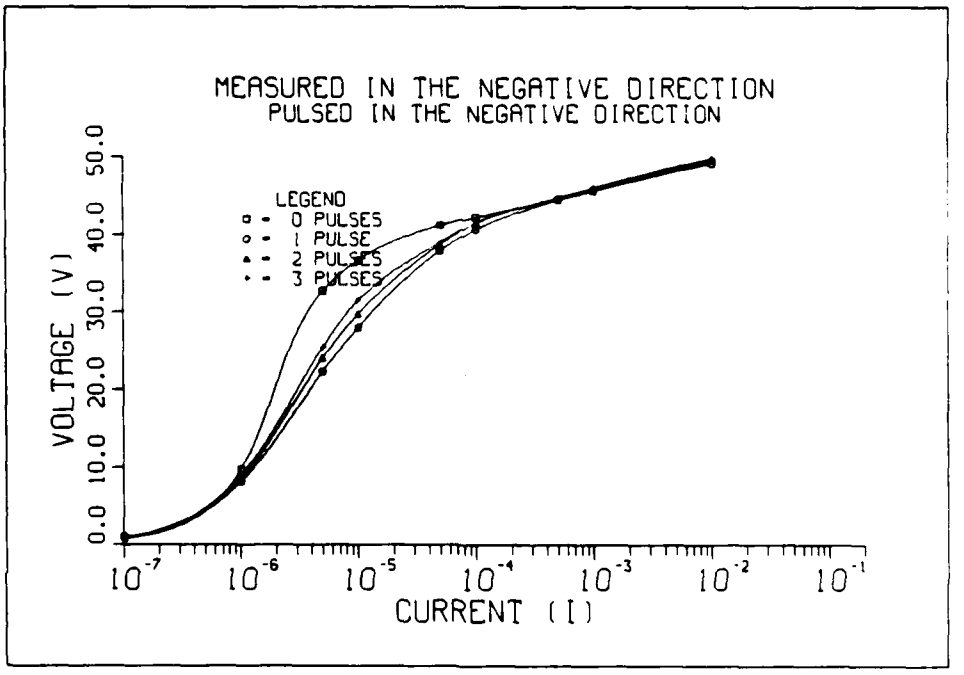

Figure A-8. I-V curves for varistor 23.

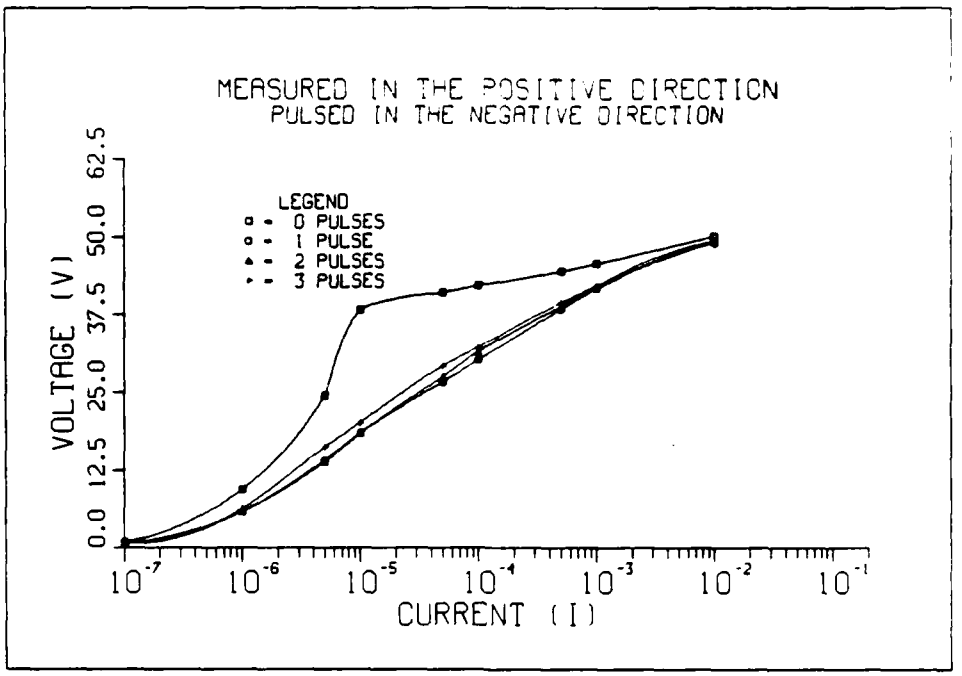

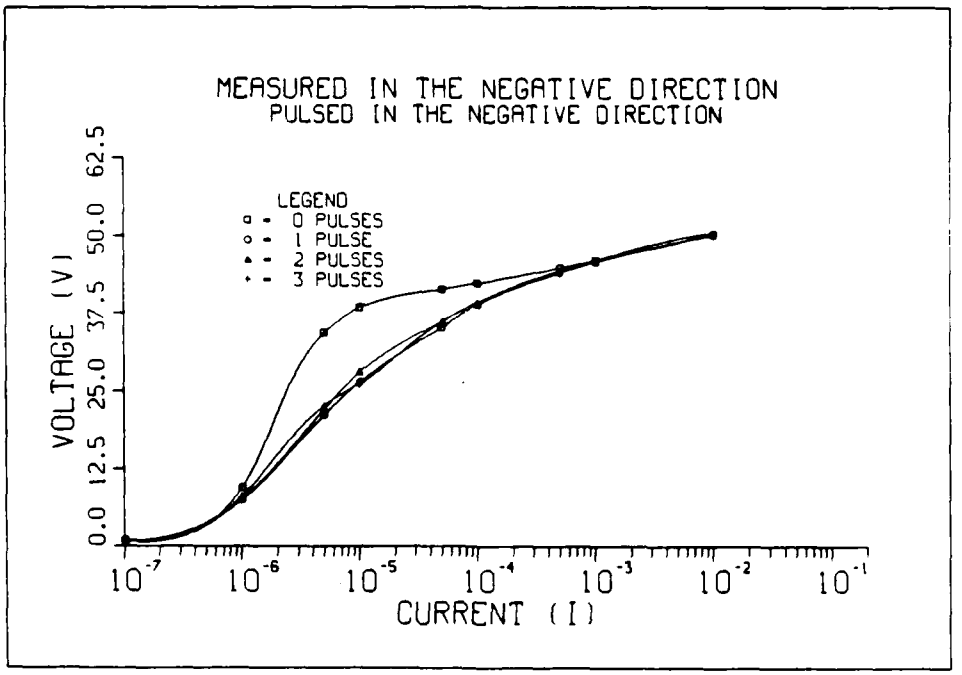

Figure A-9. I-V curves for varistor 24.

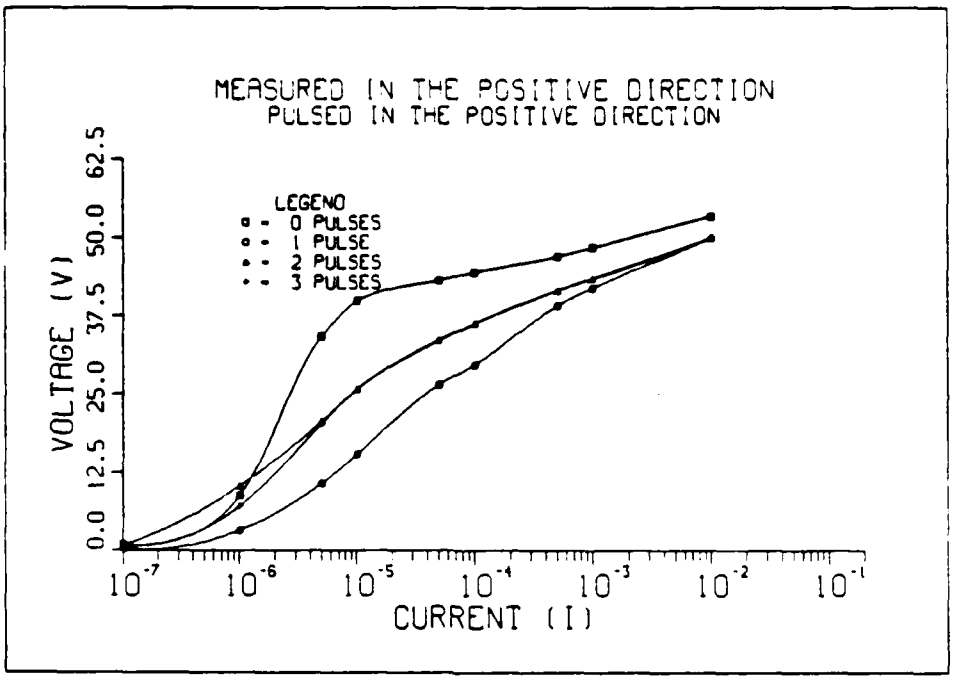

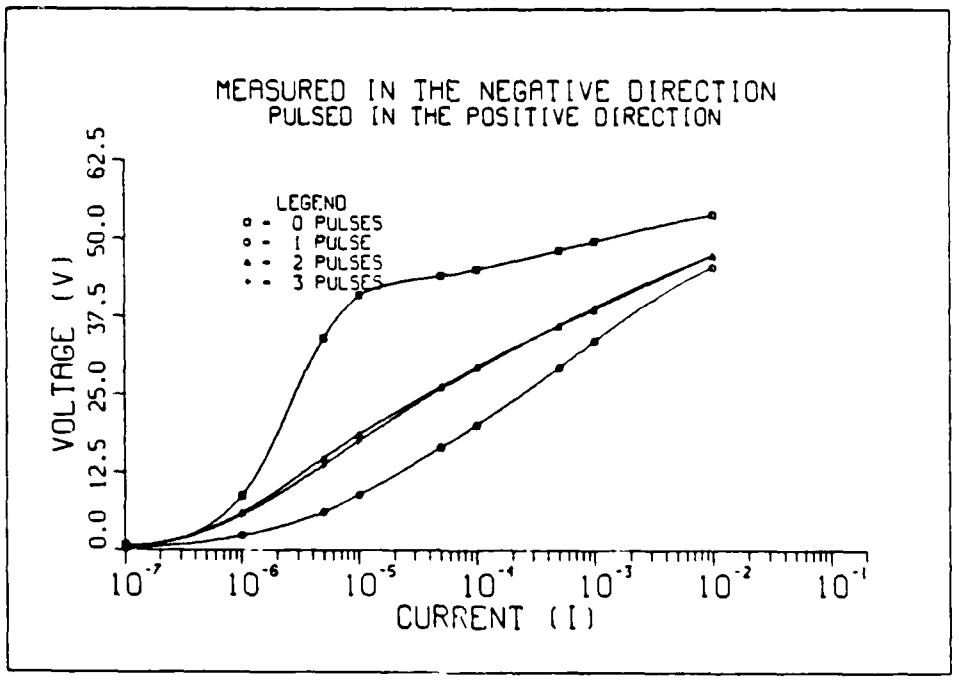

Figure A-10. I-V curves for varistor 25.

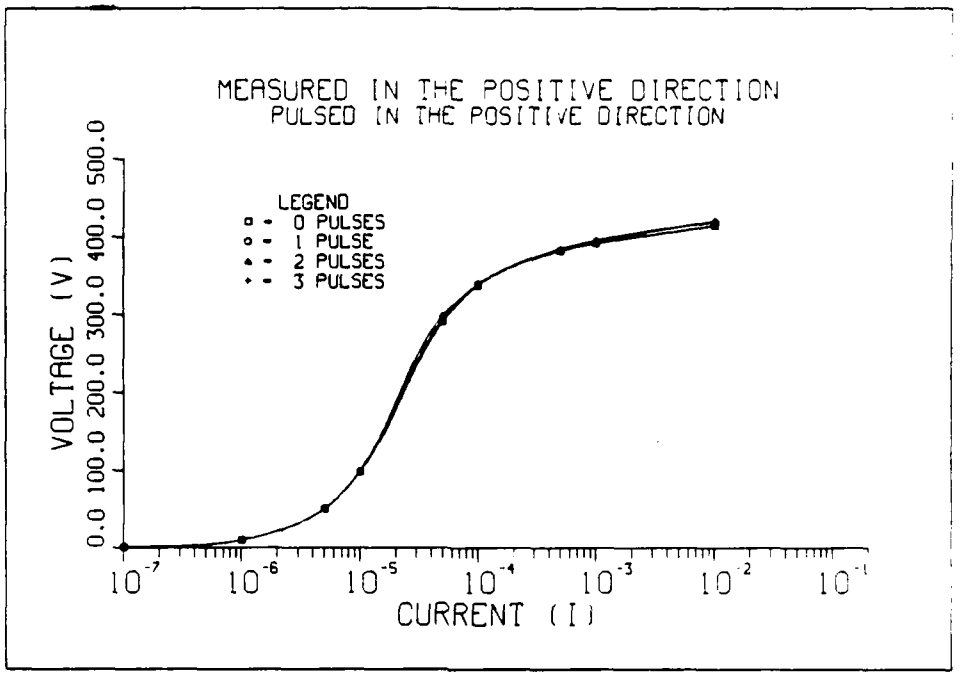

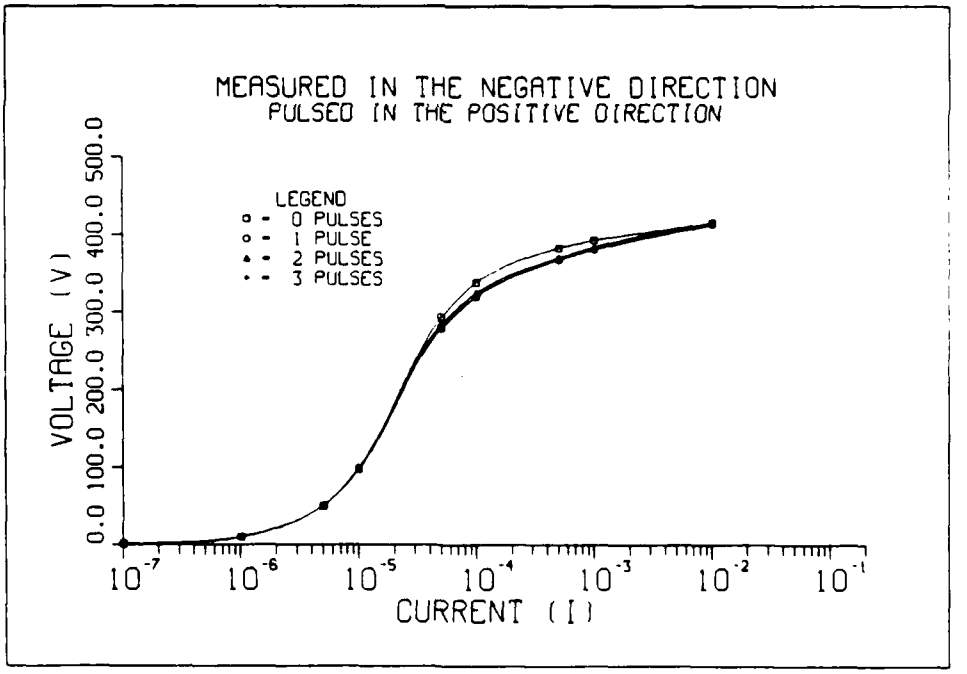

Figure A-11. I-V curves for varistor 30.

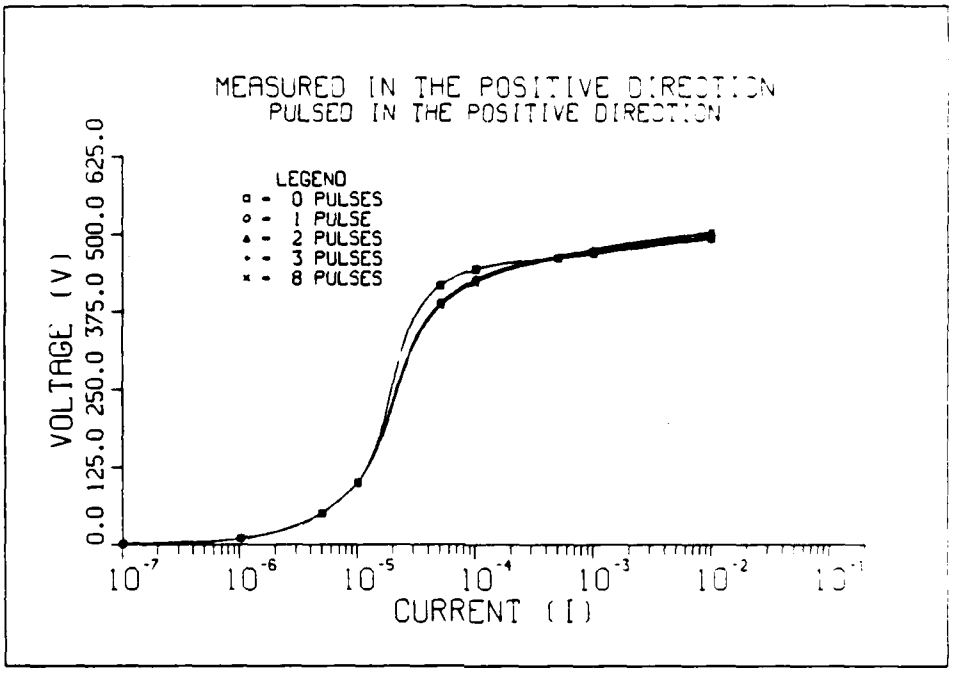

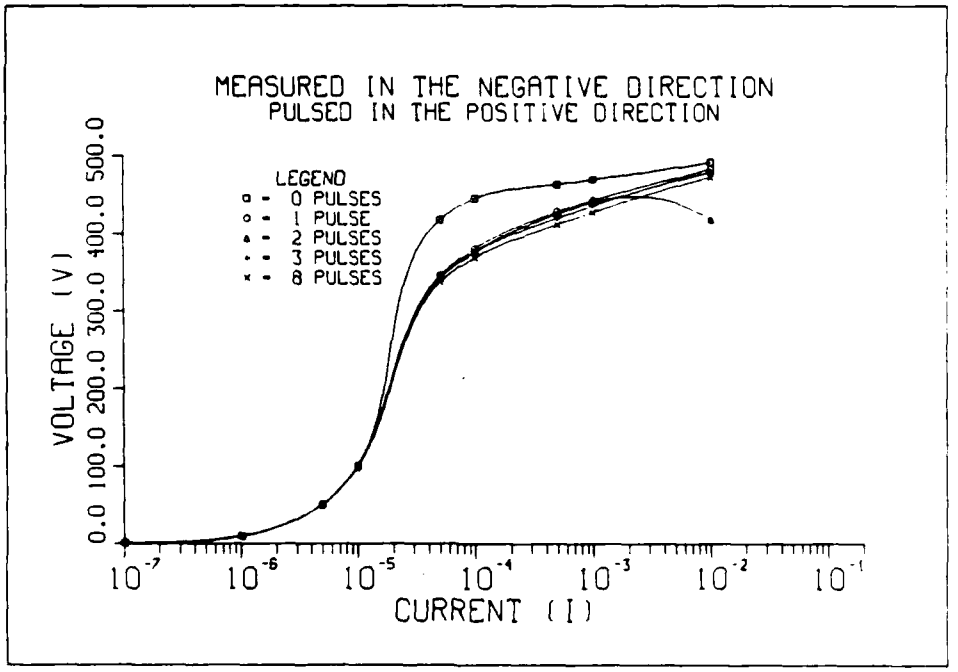

Figure A-12. I-V curves for varistor 31.

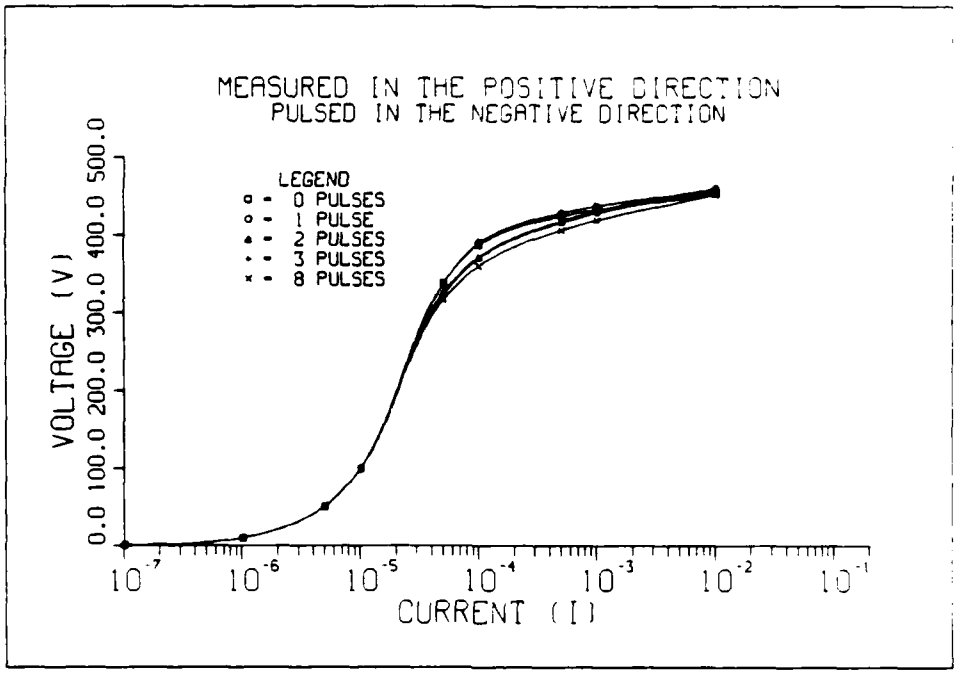

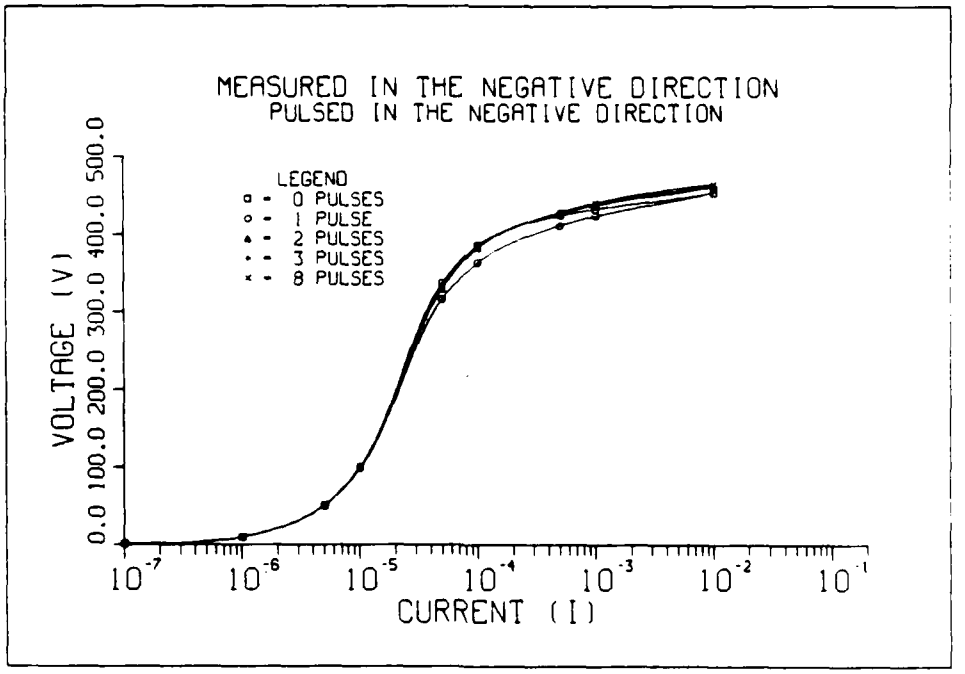

Figure A-13. I-V curves for varistor 32.

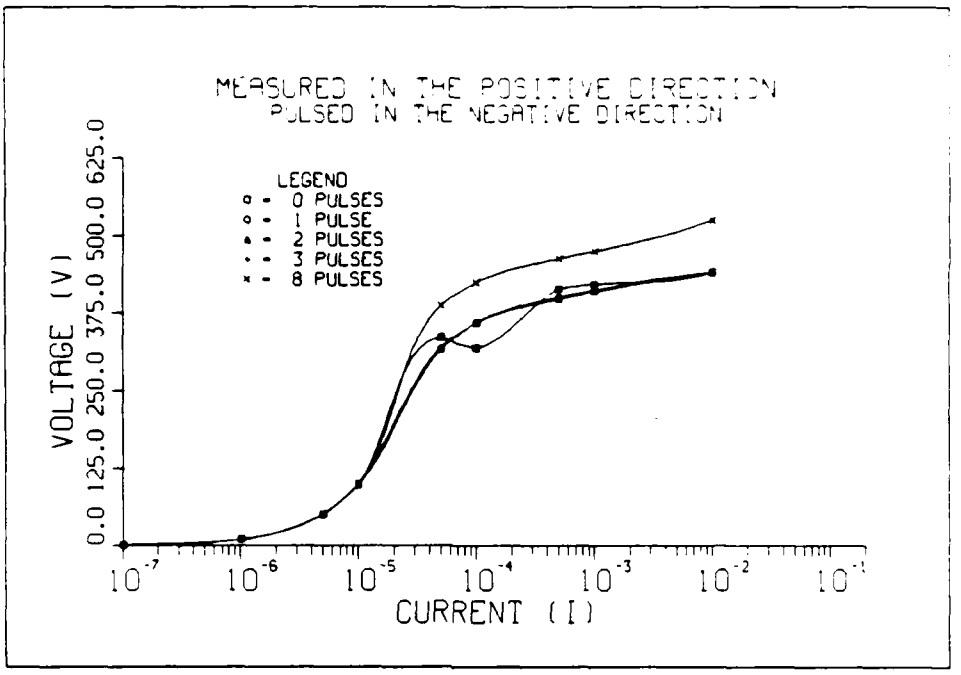

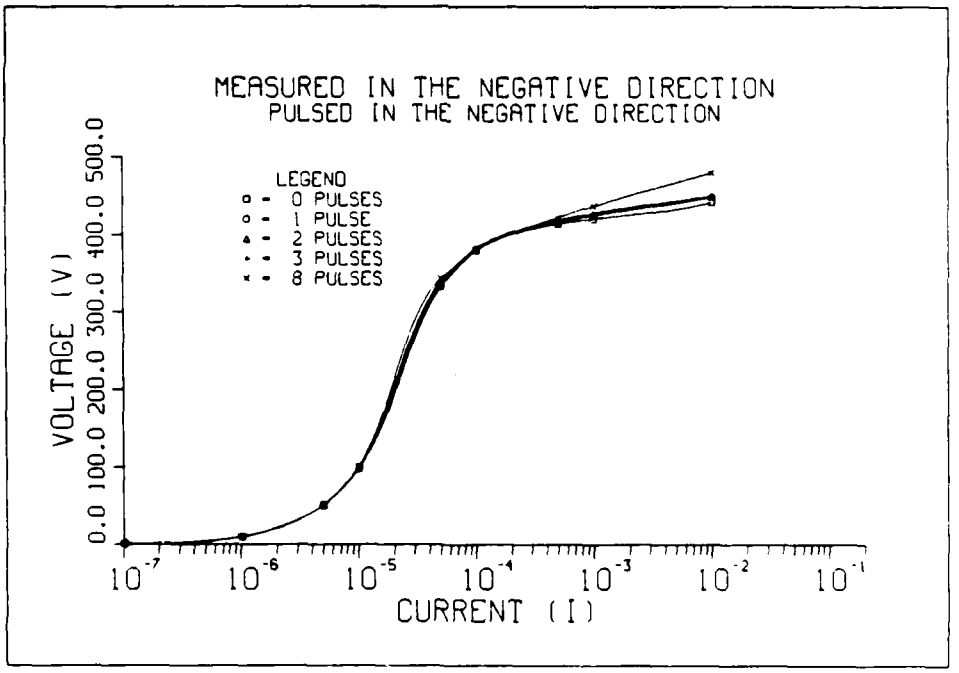

Figure A-14. I-V curves for varistor 33.

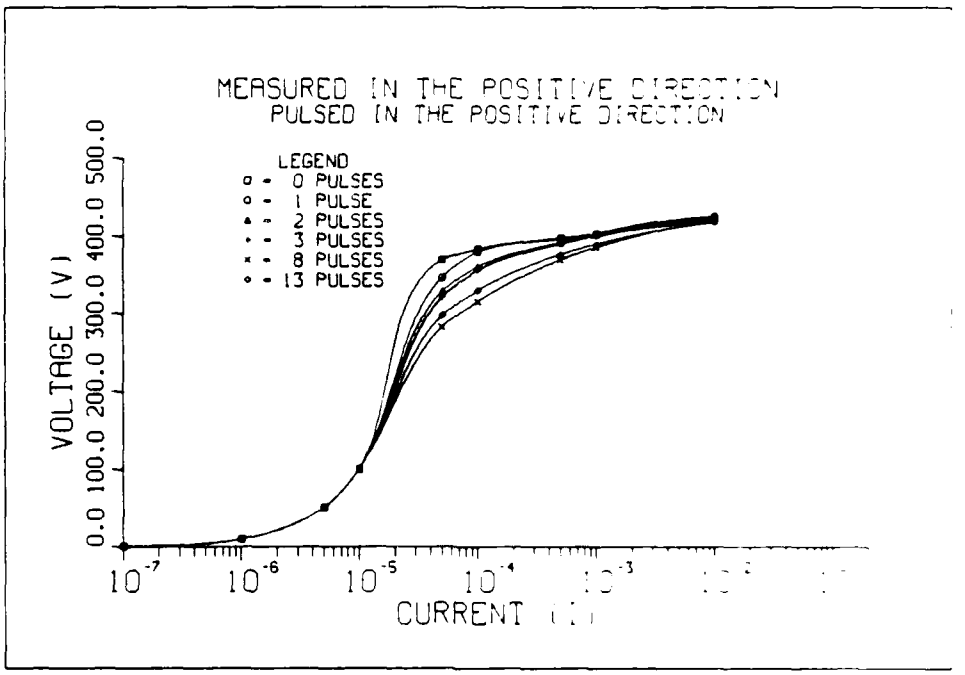

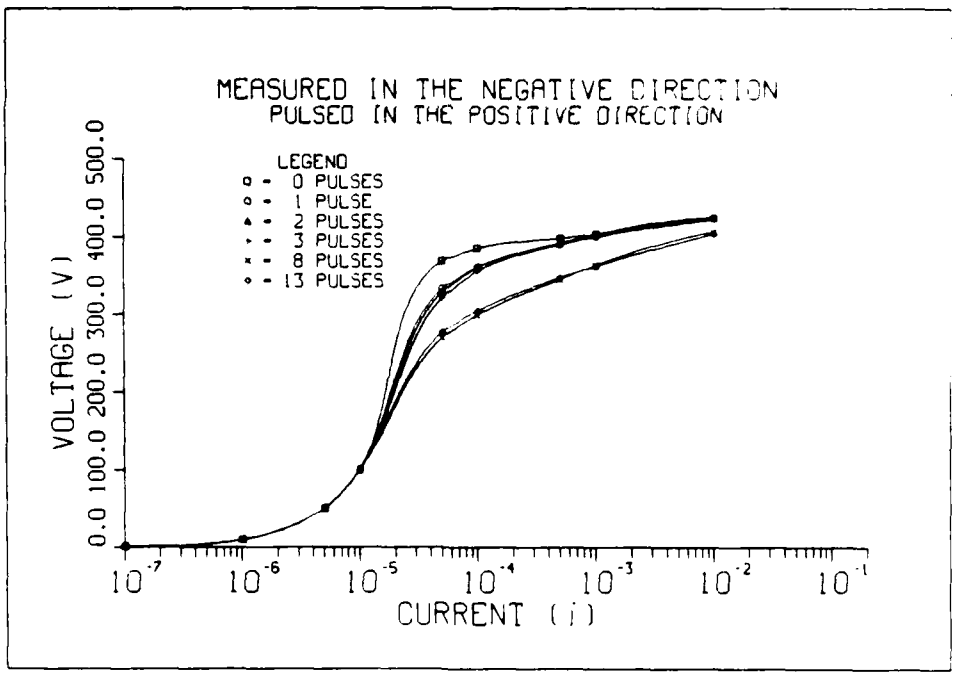

Figure A-15. I-V curves for varistor 40.

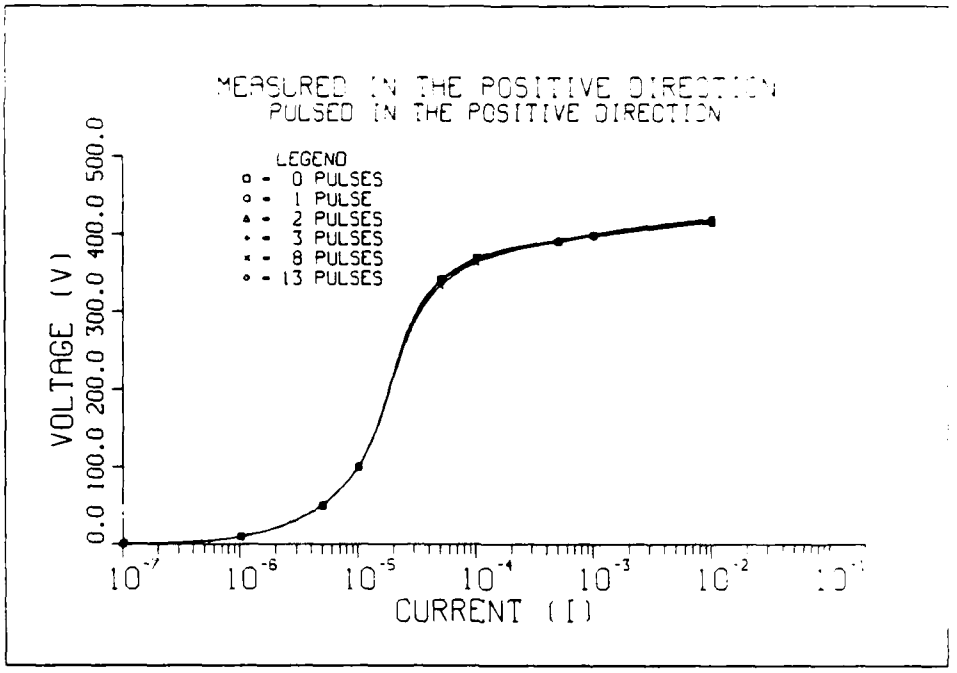

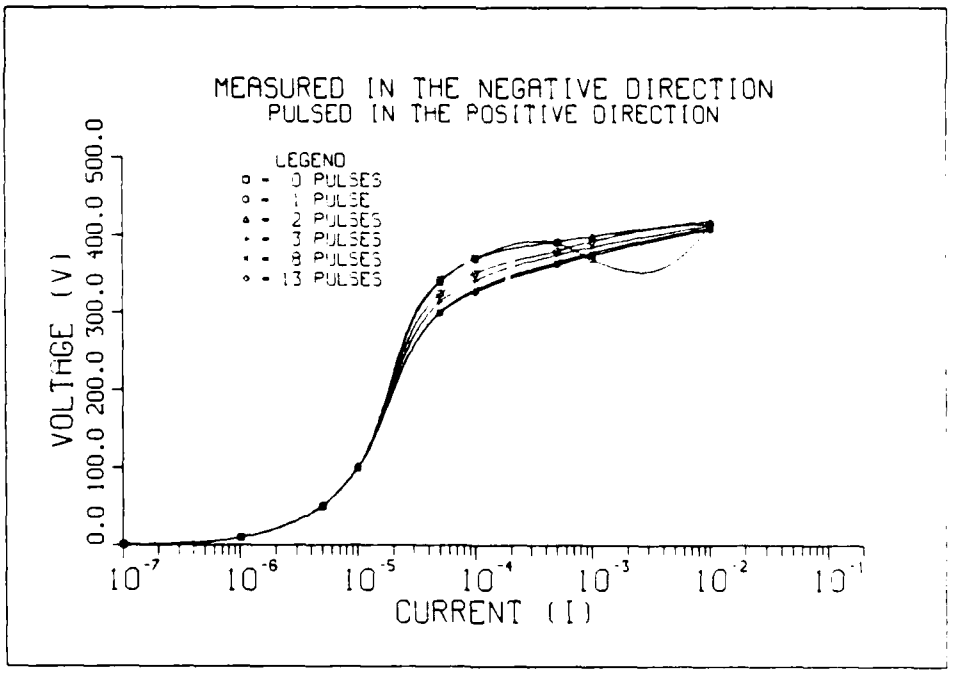

Figure A-16. I-V curves for varistor 41.

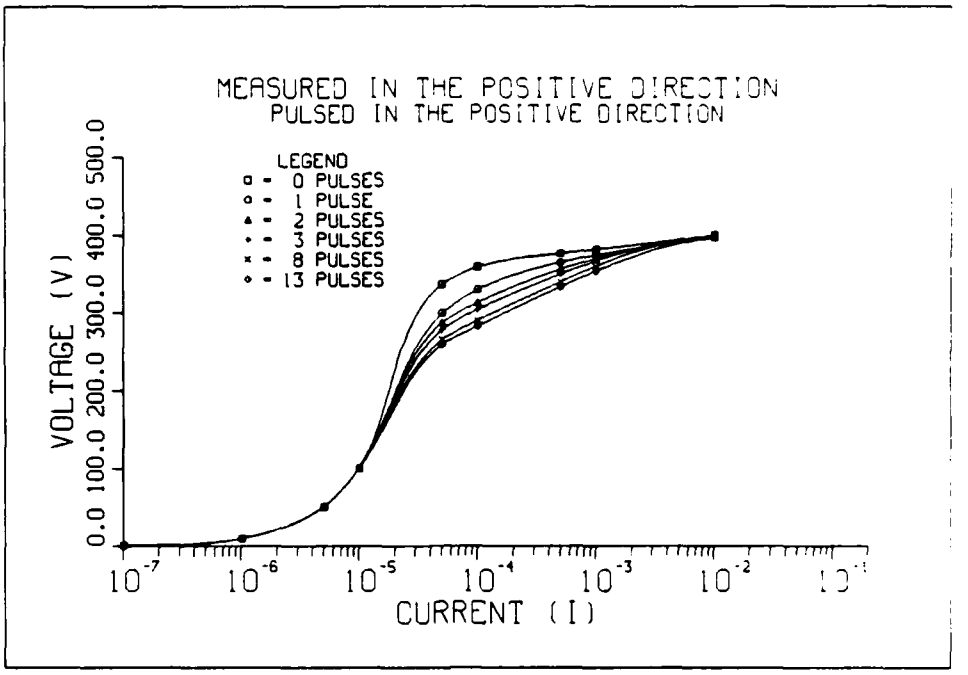

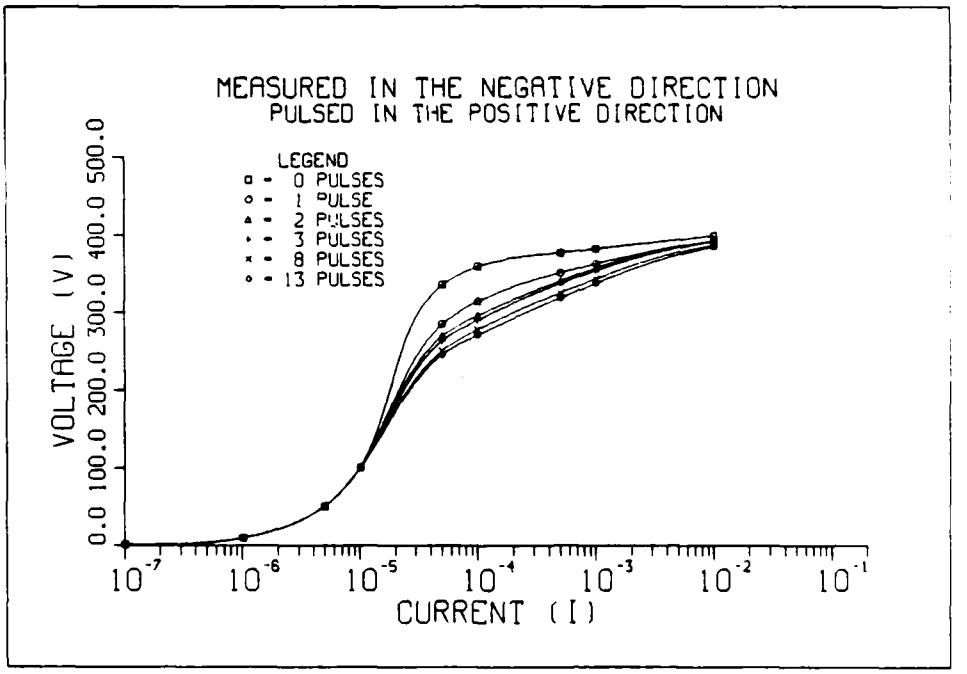

Figure A-17. I-V curves for varistor 42.

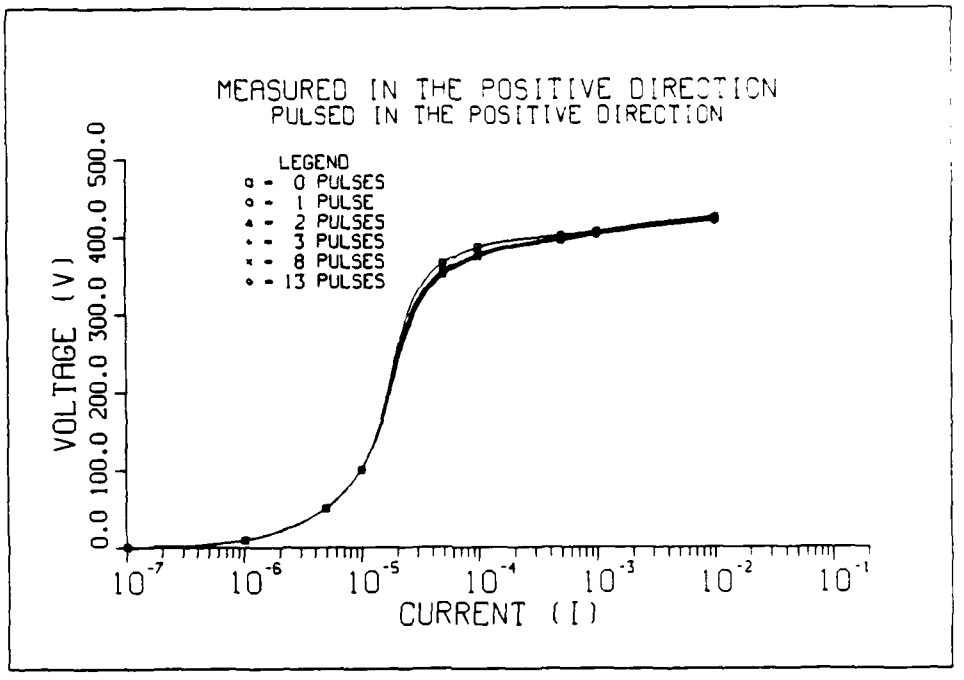

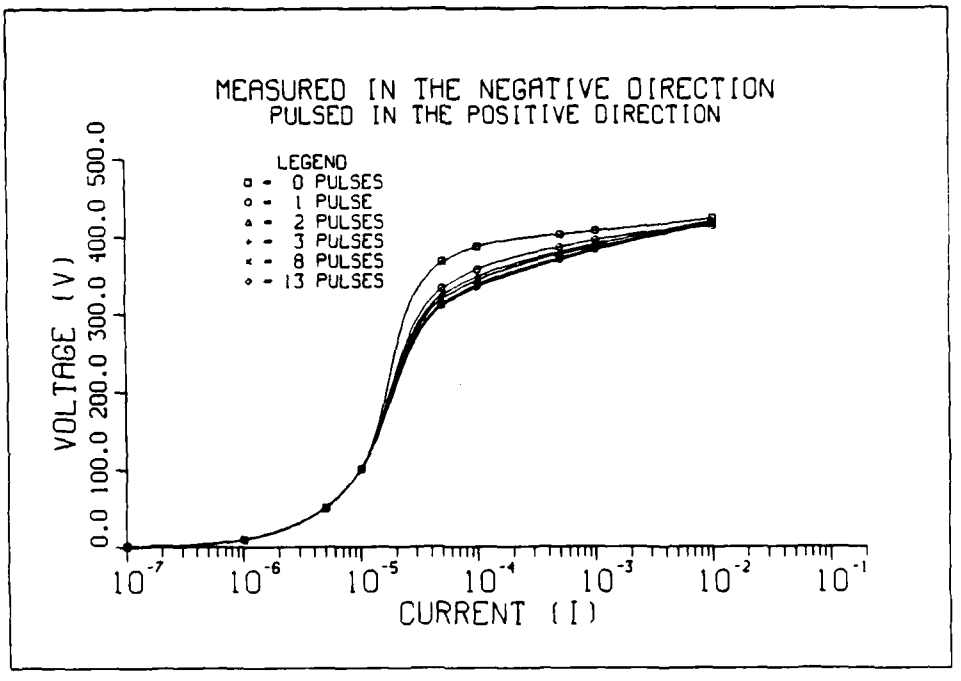

Figure A-18. I-V curves for varistor 43.

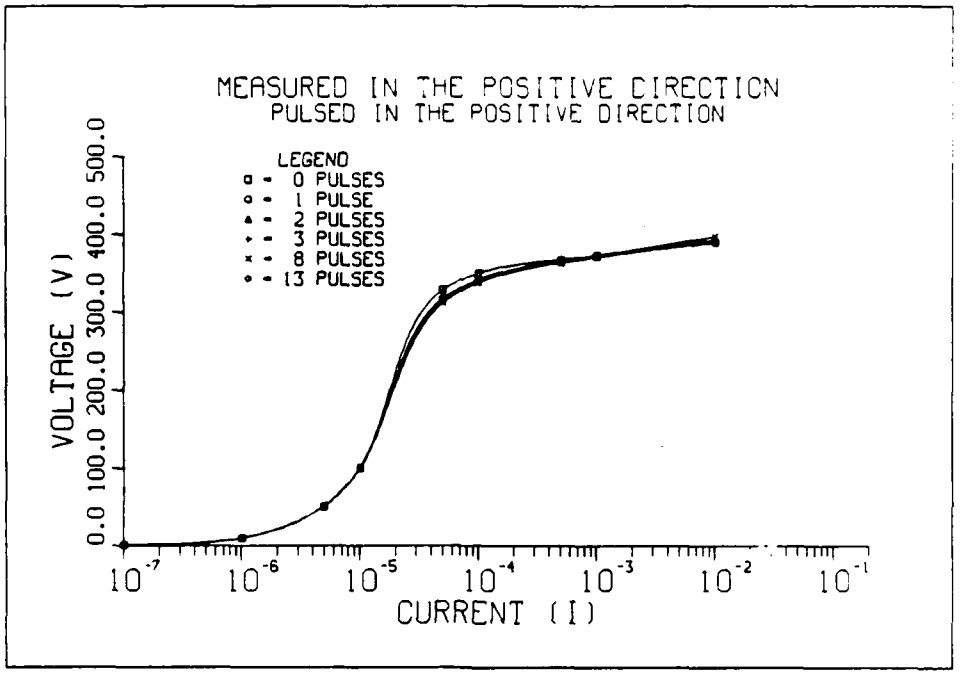

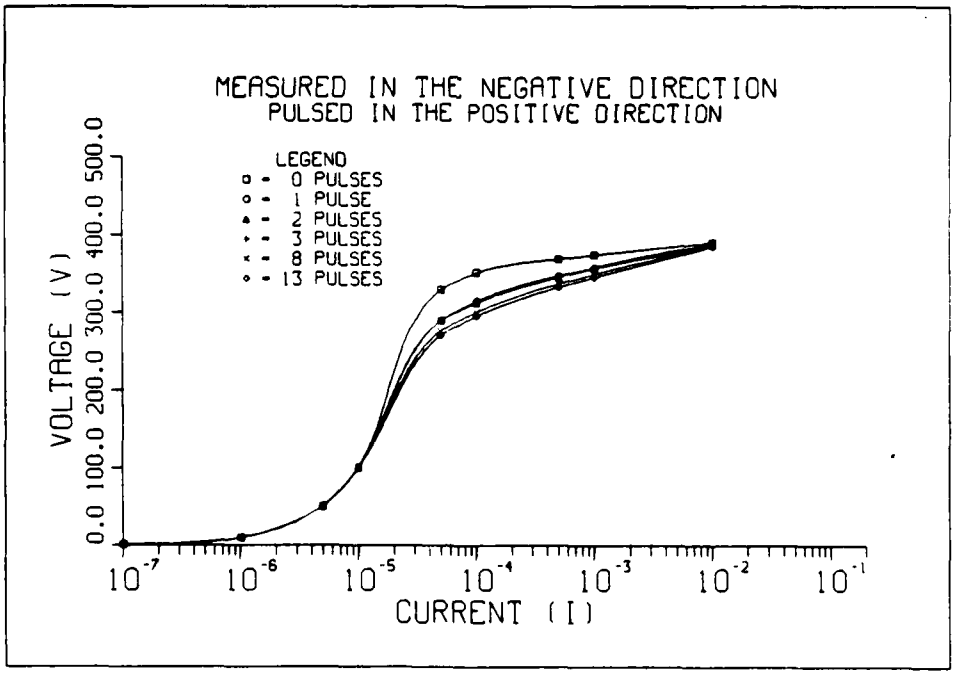

Figure A-19. I-V curves for varistor 44.

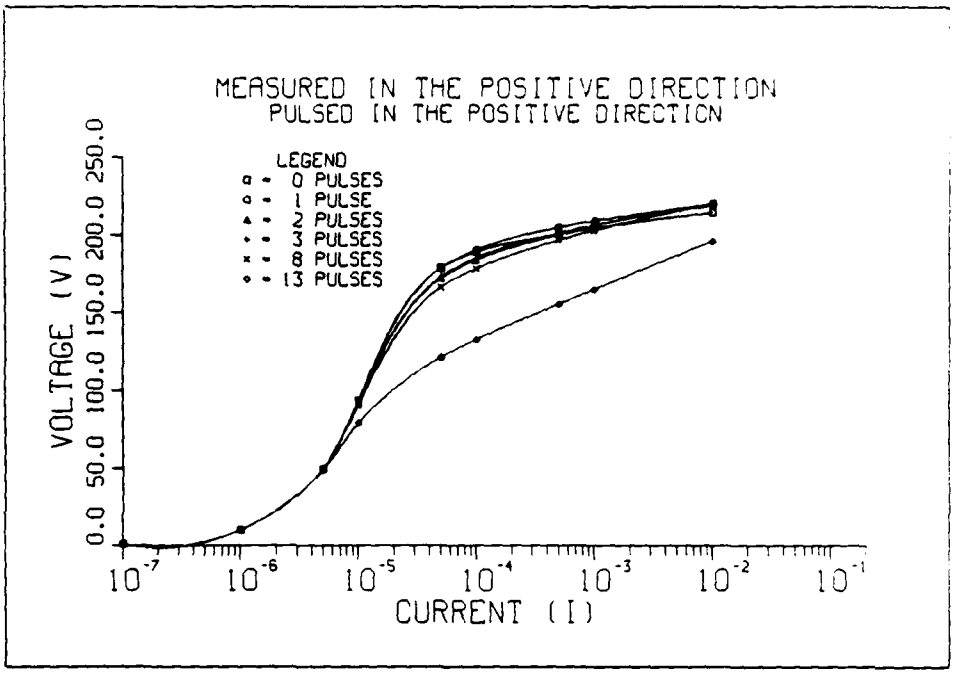

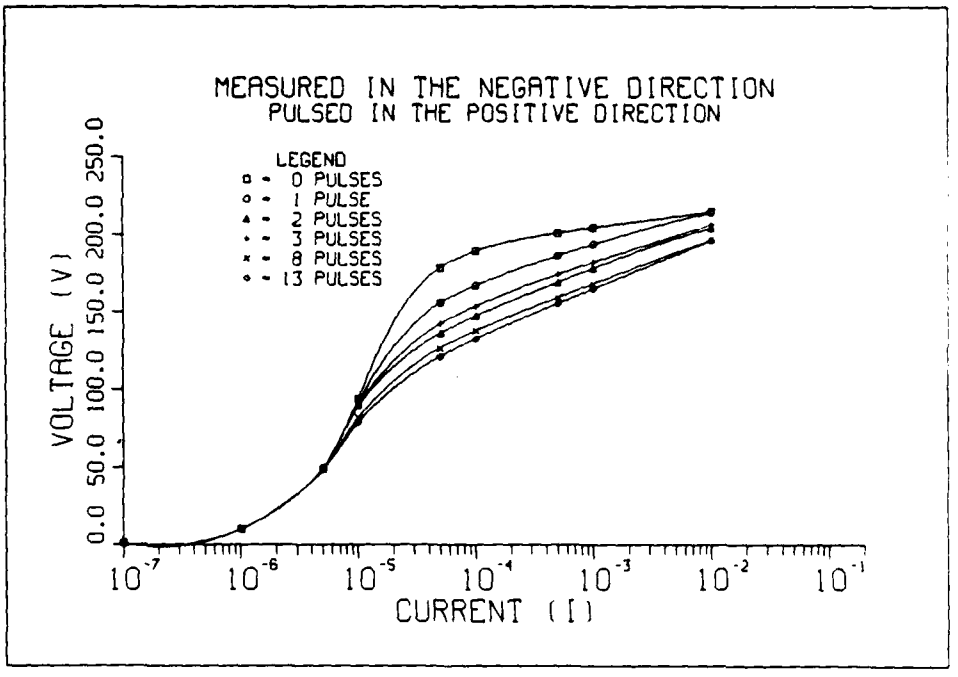

Figure A-20. I-V curves for varistor 50.

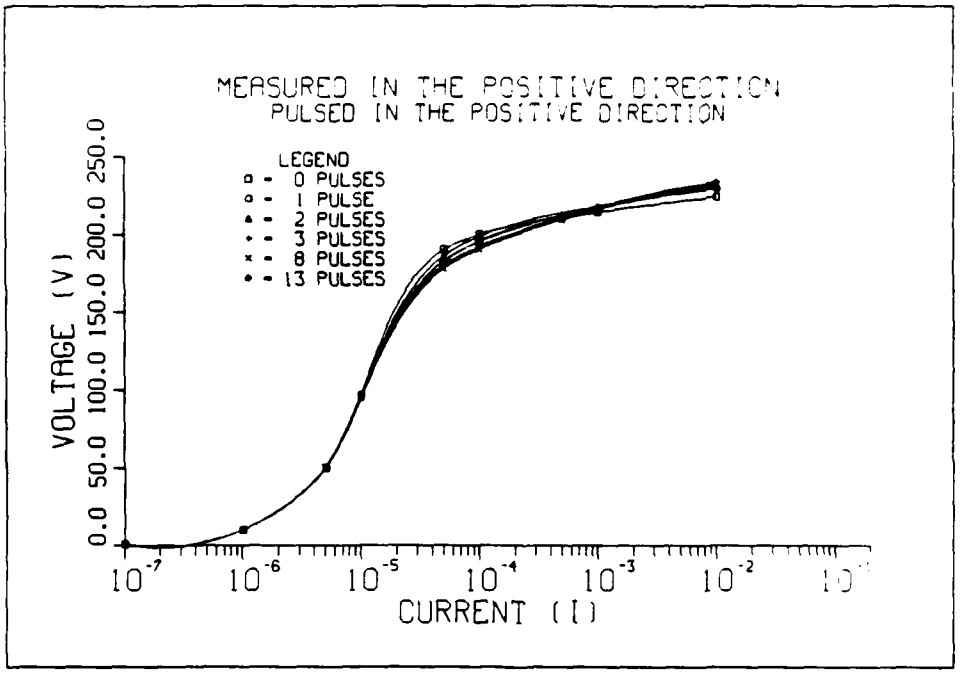

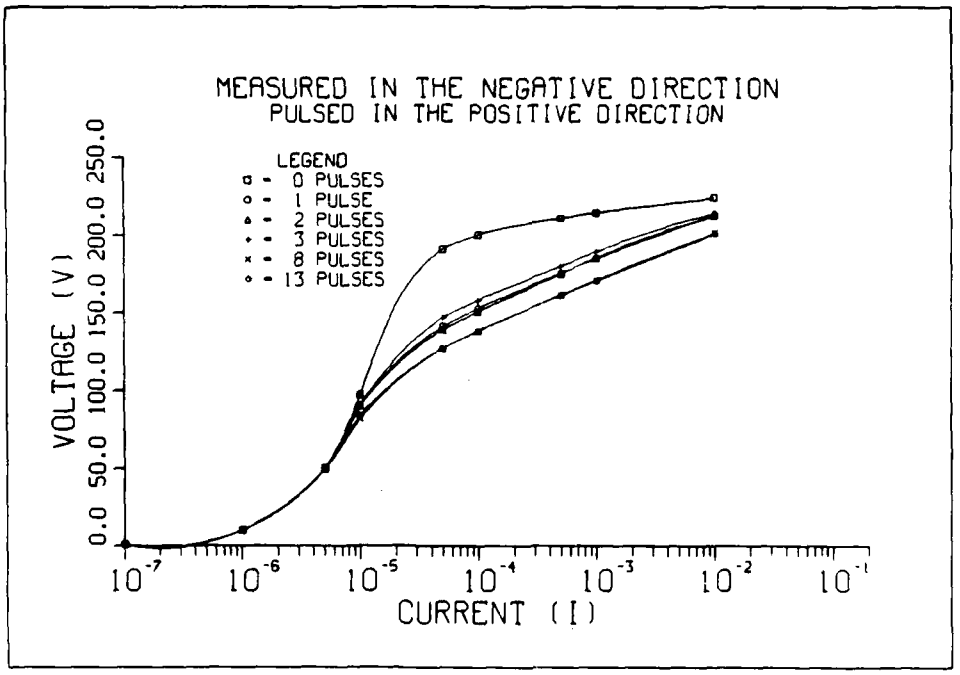

Figure A-21. I-V curves for varistor 51.

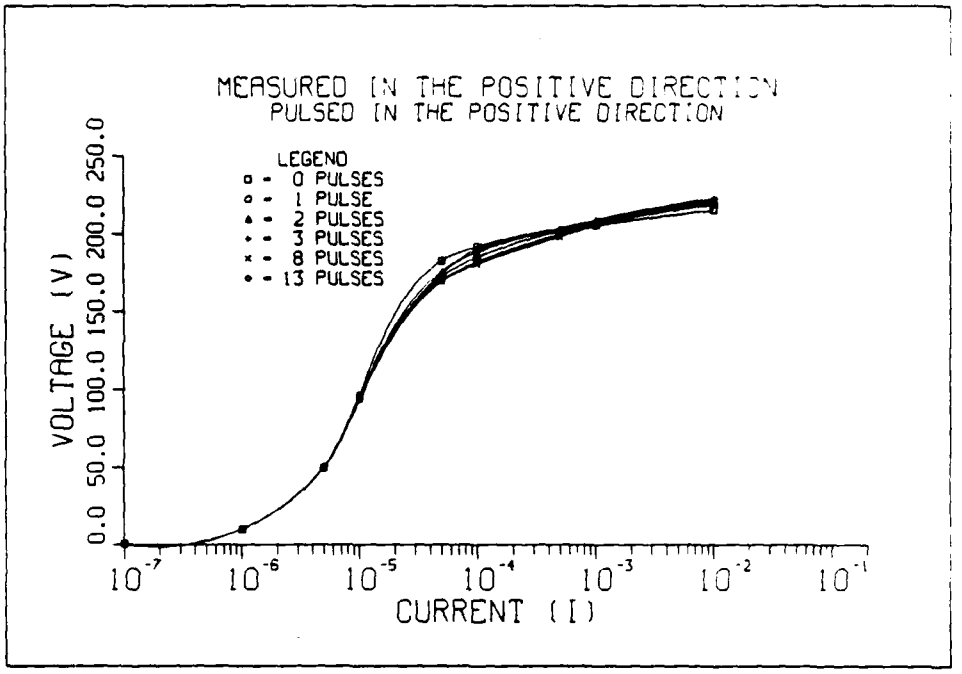

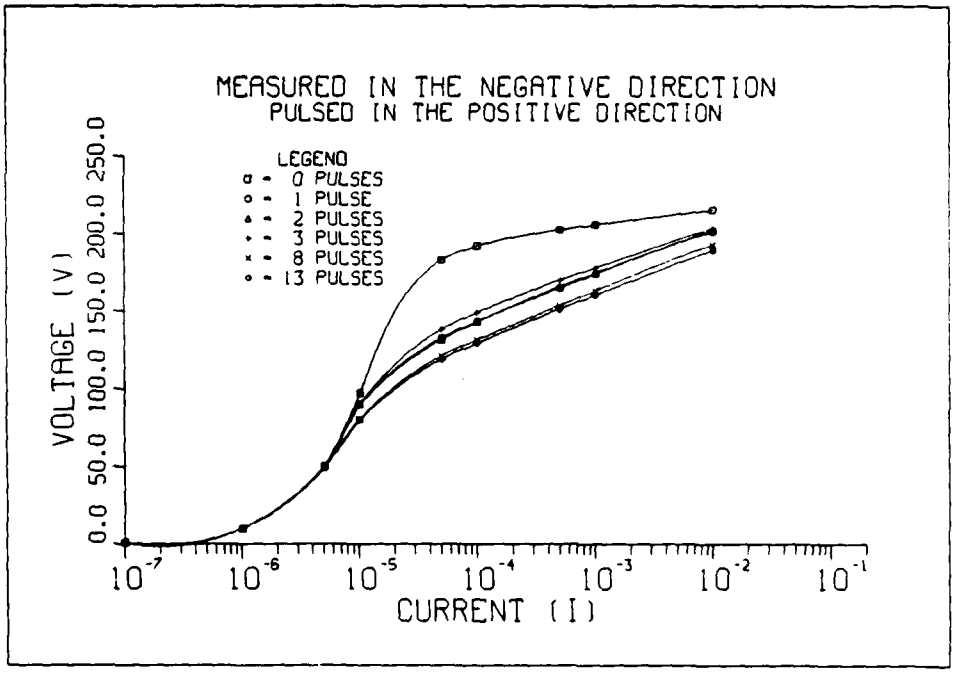

Figure A-22. I-V curves for varistor 52.

APPENDIX B

VARISTOR CLAMPING VOLTAGE CURVES

Appendix B contains the curves for the varistor clamping voltage, for 0.1 mA and 1 mA, as a function of the number of consecutive pulses. The curves are labeled with the varistor number and the pulsed polarity. Both positive and negative measured polarities are shown on a single plot to illustrate the additional degradation seen when the measured polarity is opposite to the pulsed polarity.

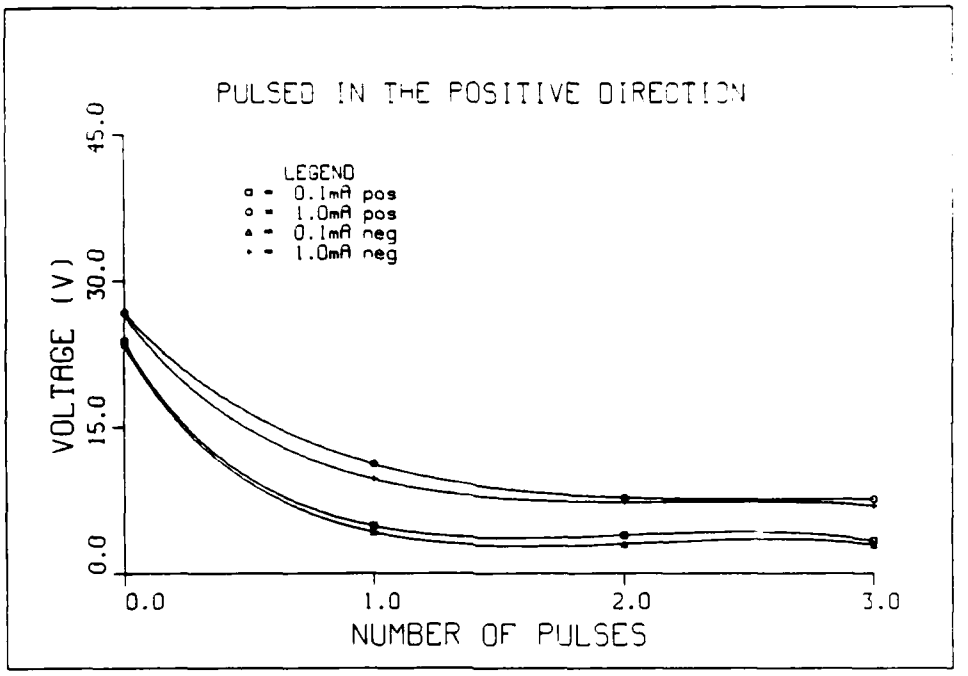

Figure B-1. Clamping voltage versus number of pulses for varistor 1.

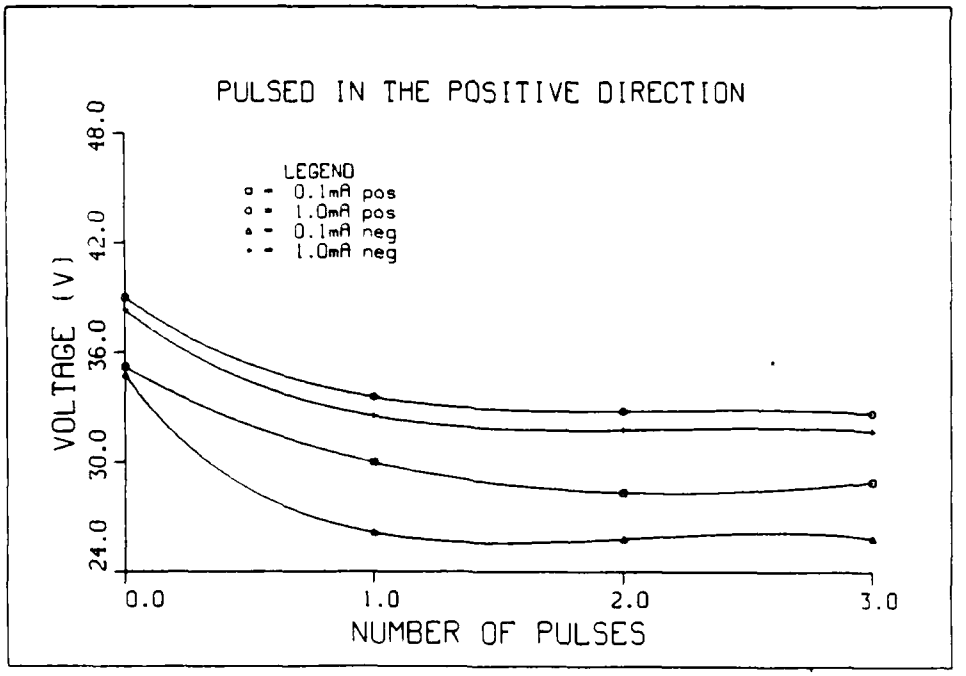

Figure B-2. Clamping voltage versus number of pulses for varistor 2.

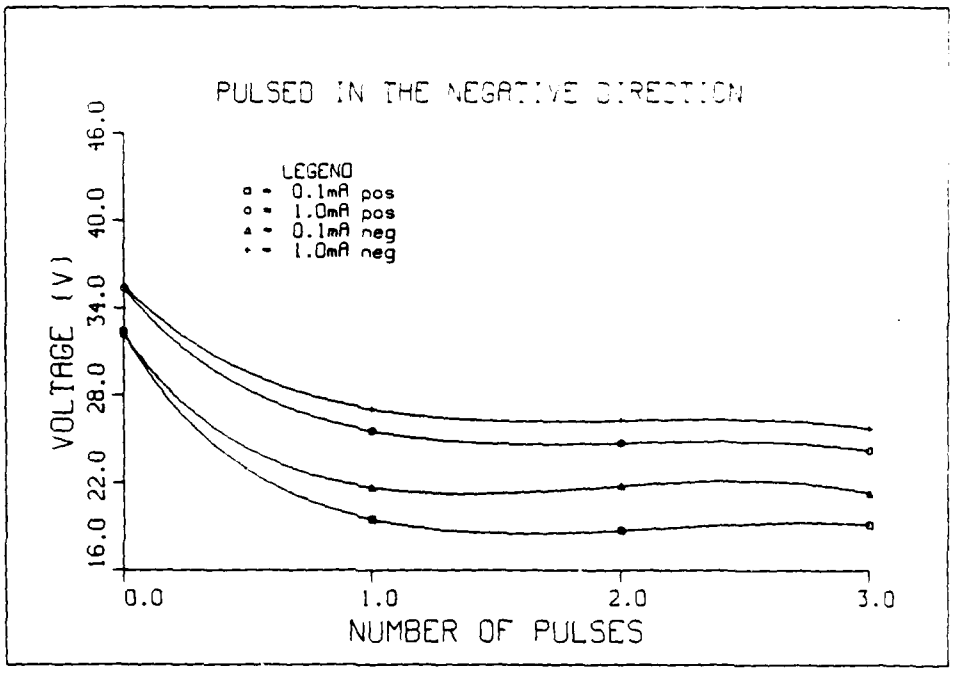

Figure B-3. Clamping voltage versus number of pulses for varistor 3.

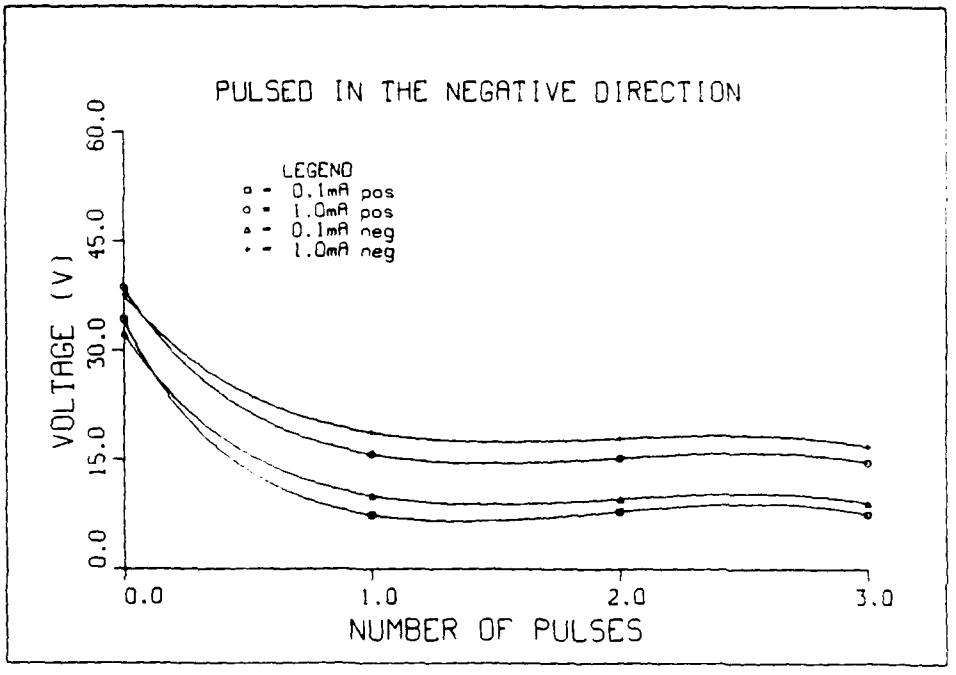

Figure B-4. Clamping voltage versus number of pulses for varistor 4.

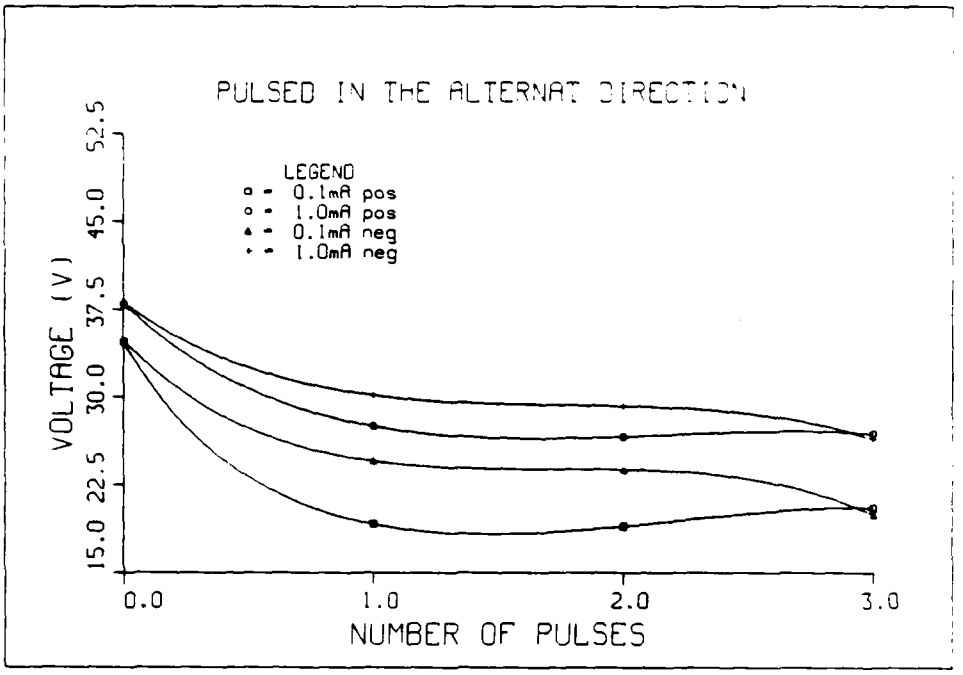

Figure B-5. Clamping voltage versus number of pulses for varistor 5.

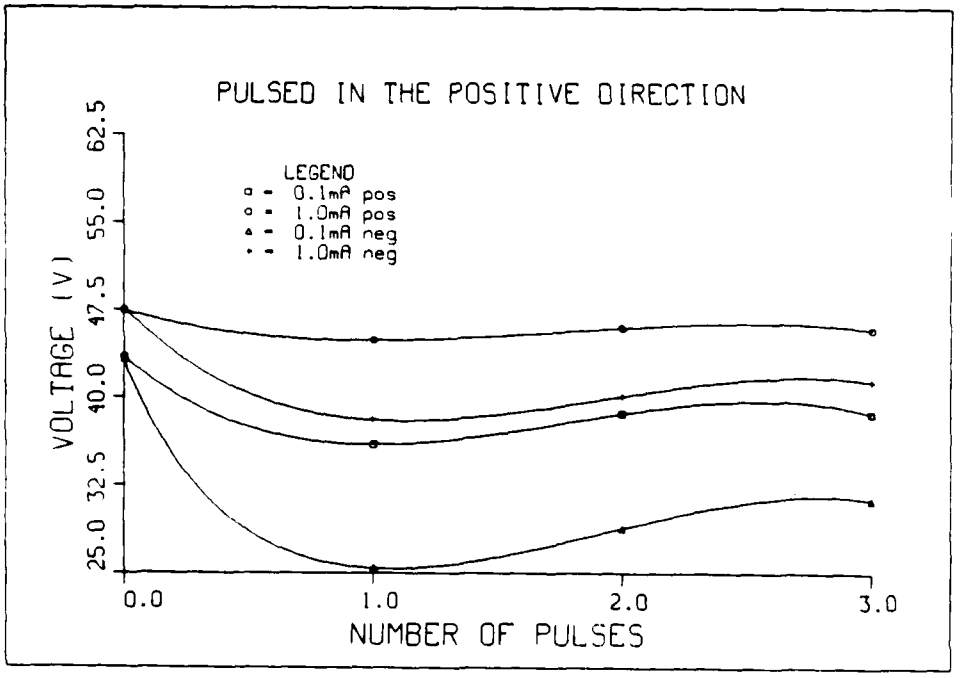

Figure B-6. Clamping voltage versus number of pulses for varistor 21.

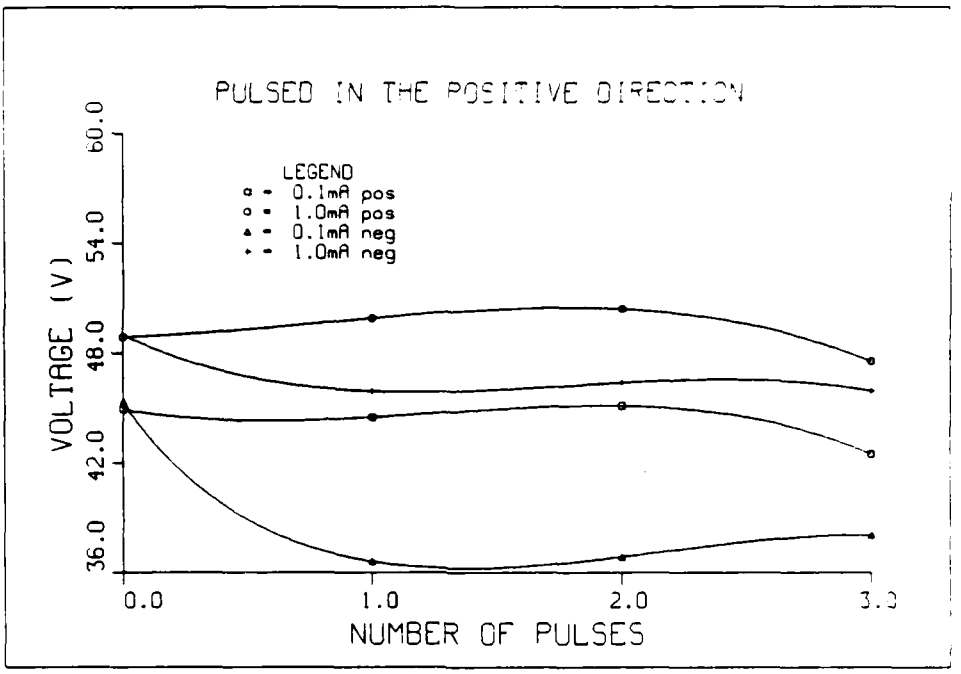

Figure B-7. Clamping voltage versus number of pulses for varistor 22.

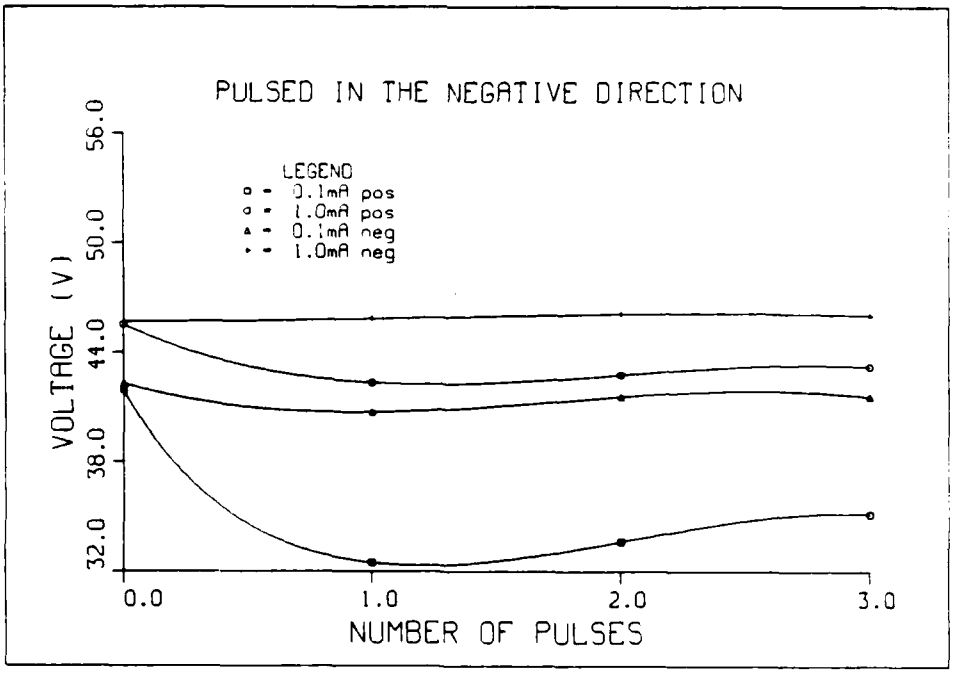

Figure B-8. Clamping voltage versus number of pulses for varistor 23.

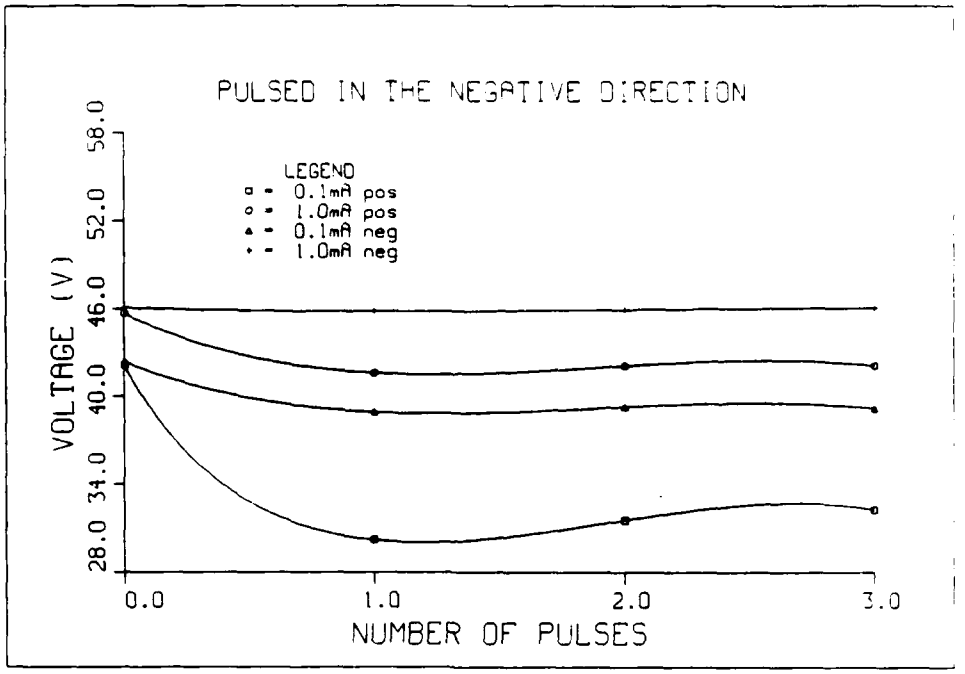

Figure B-9. Clamping voltage versus number of pulses for varistor 24.

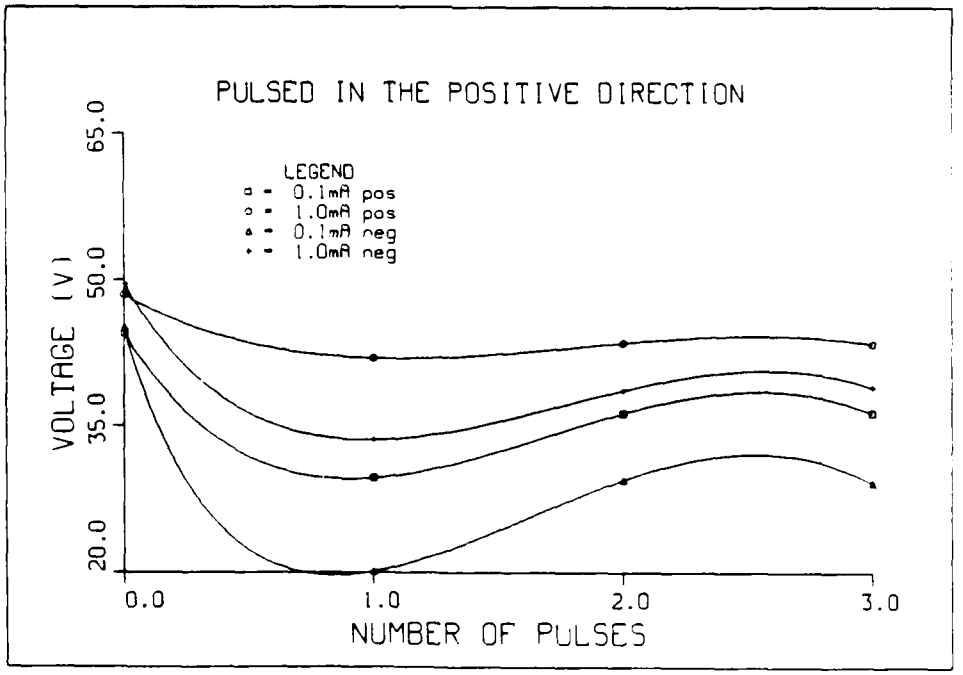

Figure B-10. Clamping voltage versus number of pulses for varistor 25.

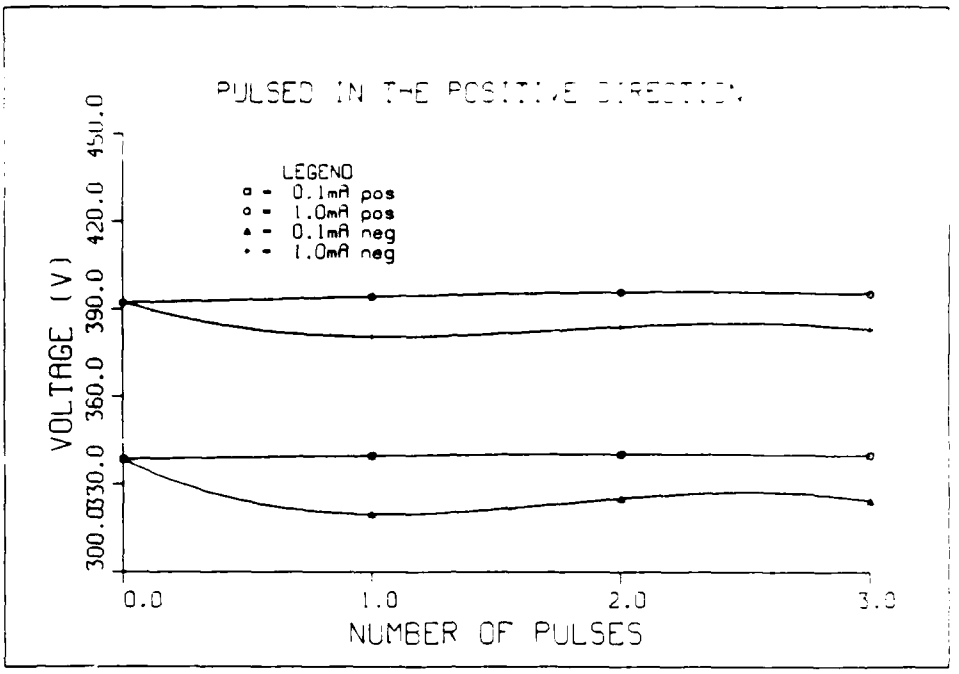

Figure B-11. Clamping voltage versus number of pulses for varistor 30.

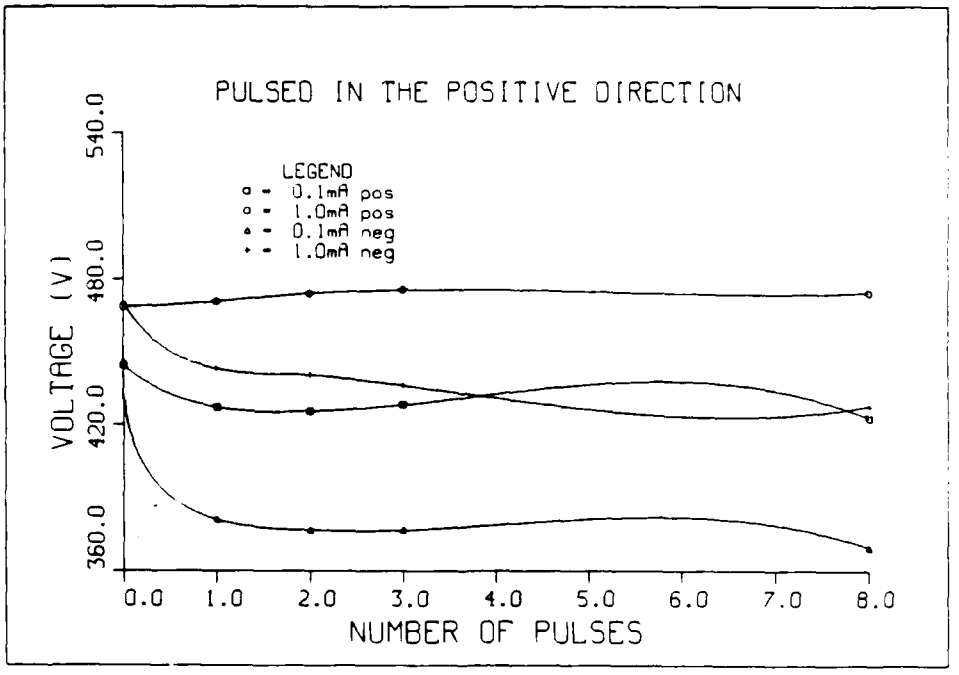

Figure B-12. Clamping voltage versus number of pulses for varistor 31.

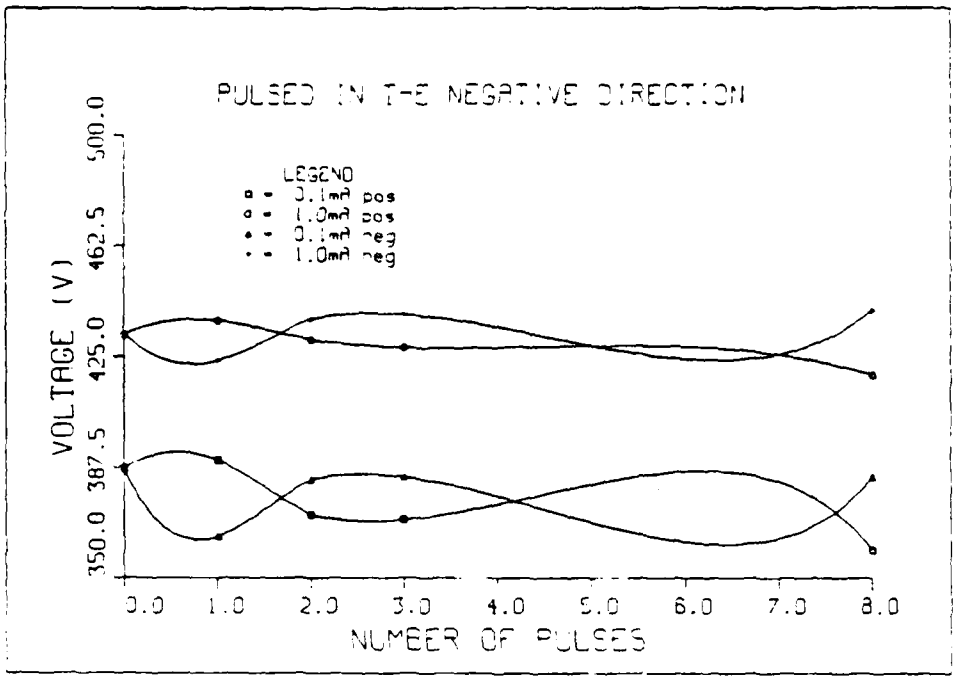

Figure B-13. Clamping voltage versus number of pulses for varistor 32.

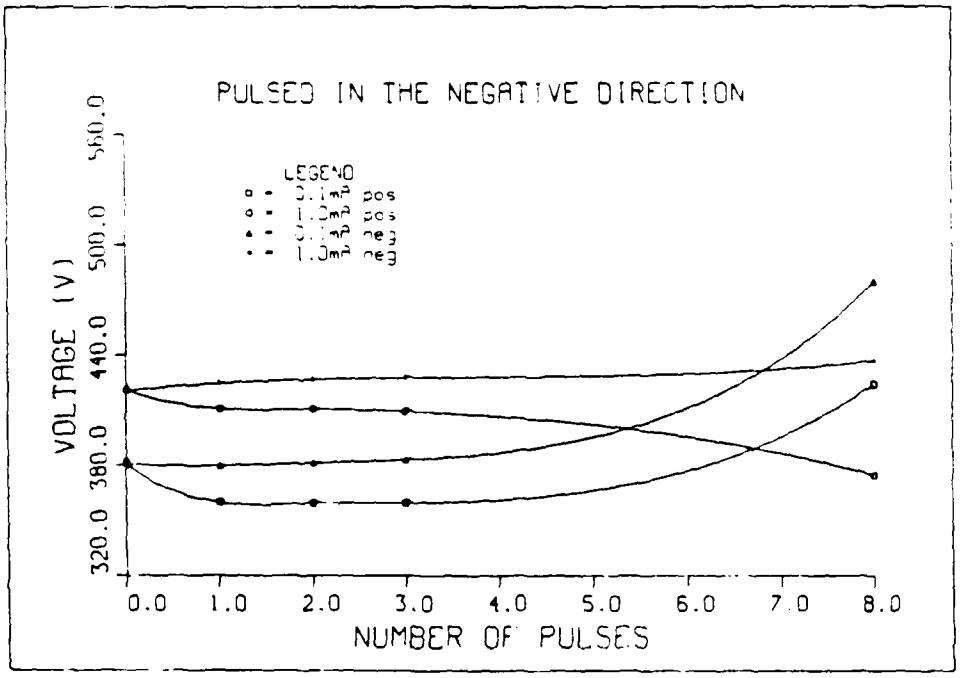

Figure B-14. Clamping voltage versus number of pulses for varistor 33.

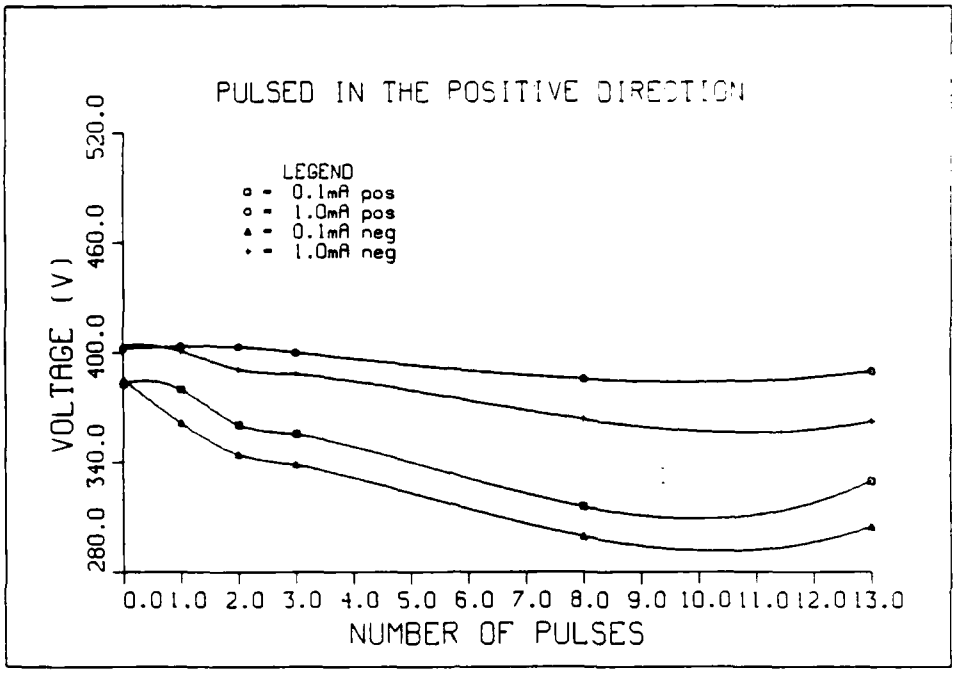

Figure B-15. Clamping voltage versus number of pulses for varistor 40.

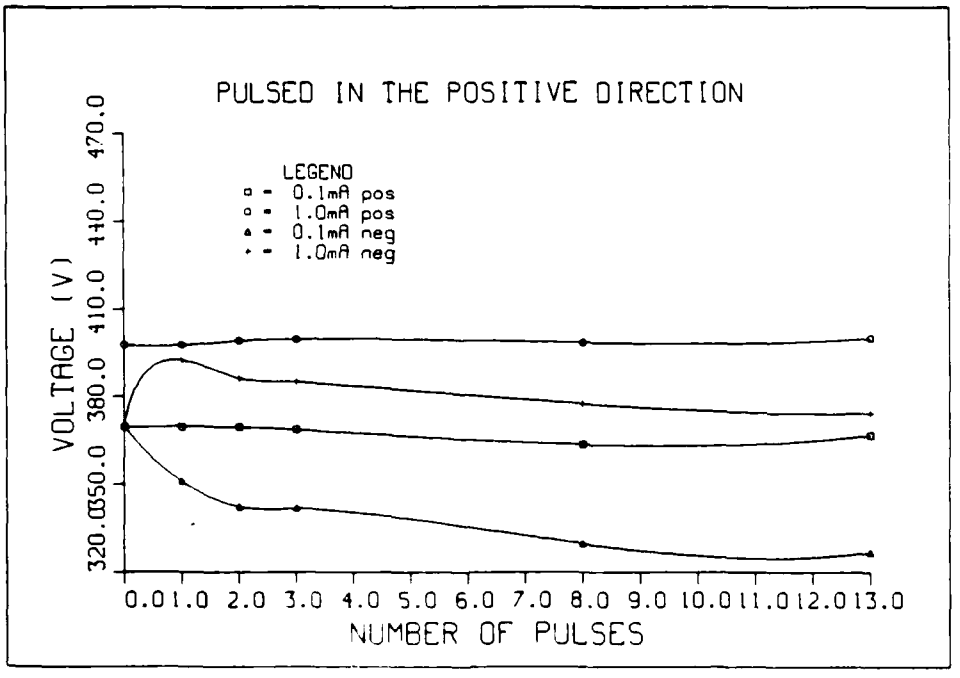

Figure B-16. Clamping voltage versus number of pulses for varistor 41.

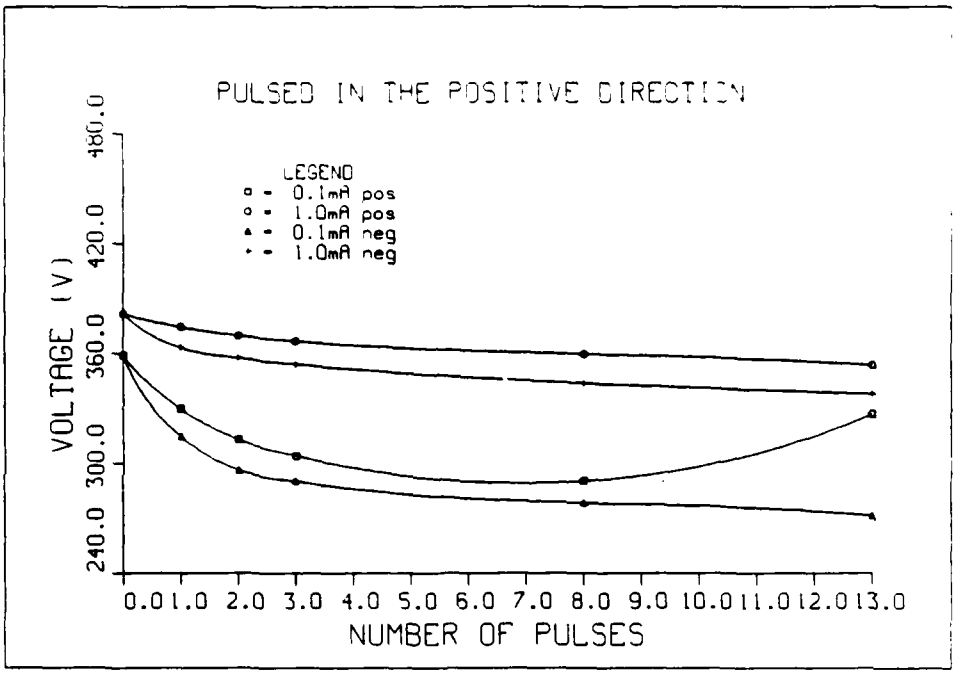

Figure B-17. Clamping voltage versus number of pulses for varistor 42.

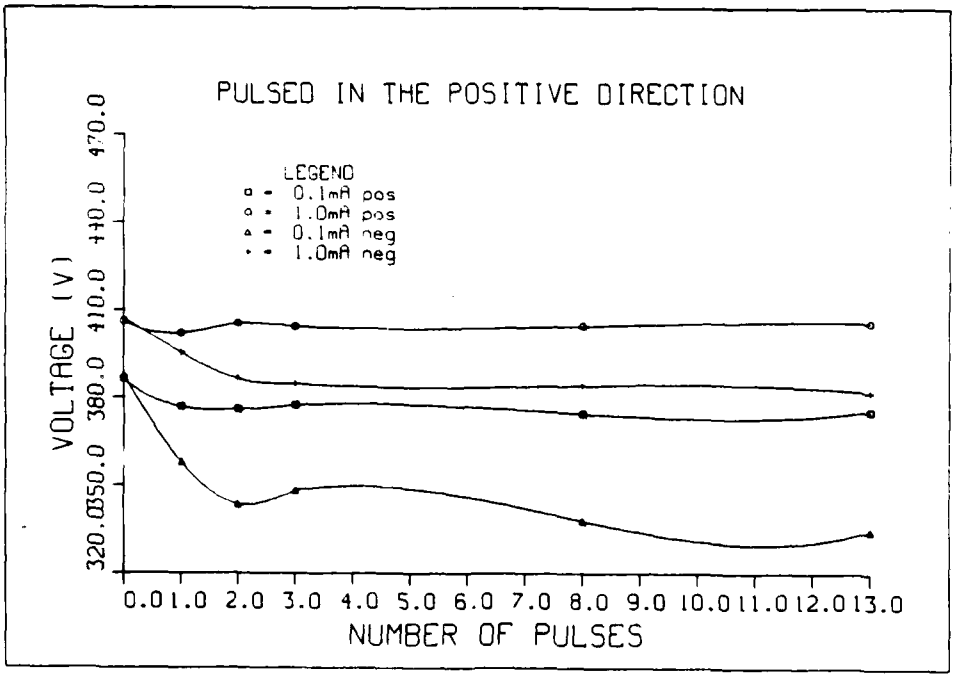

Figure B-18. Clamping voltage versus number of pulses for varistor 43.

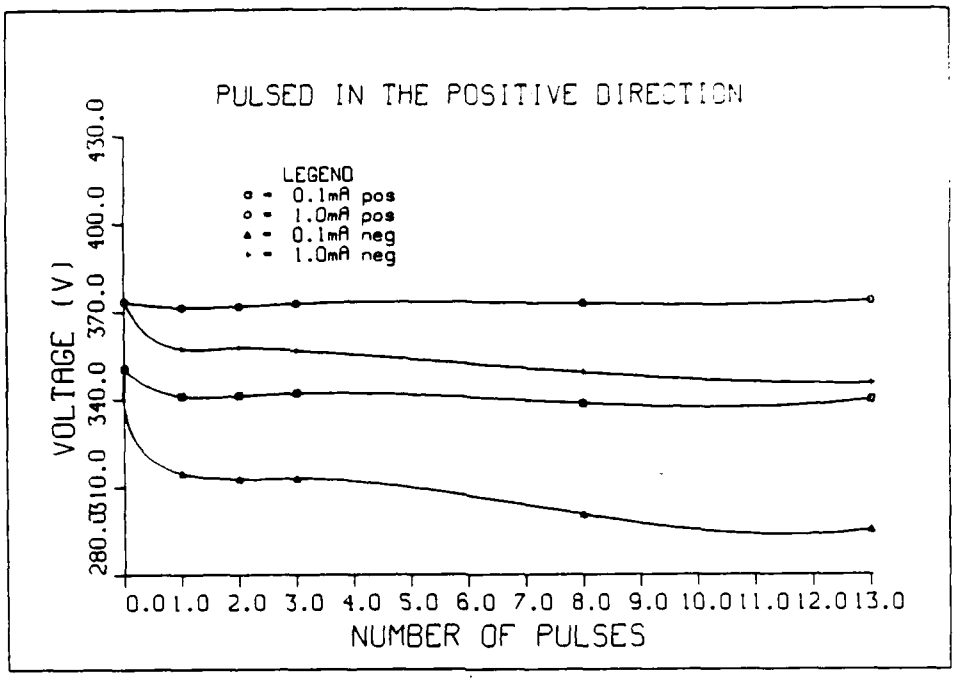

Figure B-19. Clamping voltage versus number of pulses for varistor 44.

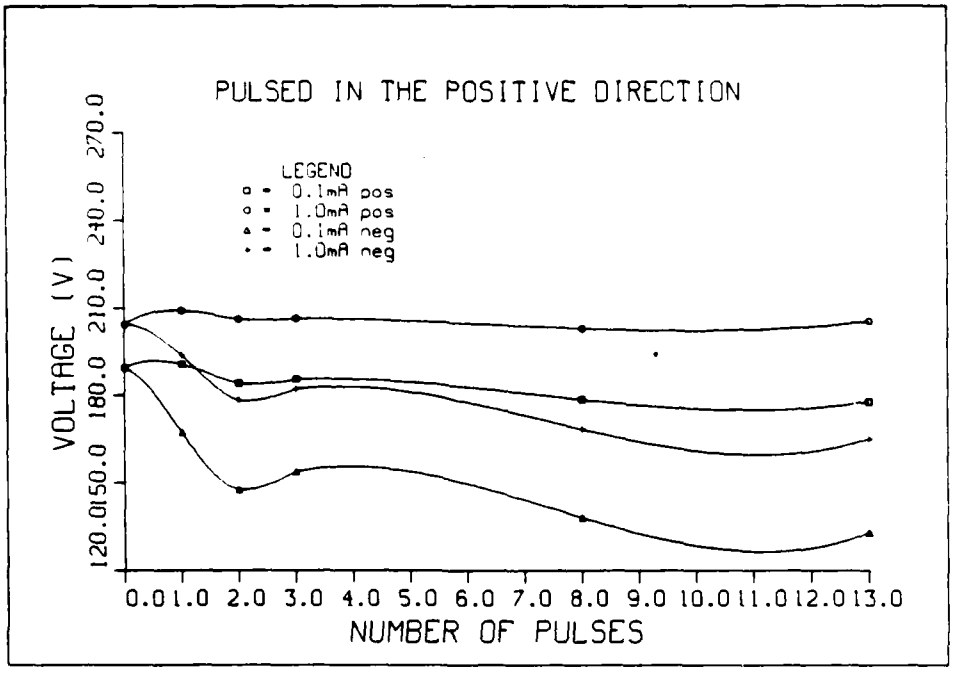

Figure B-20. Clamping voltage versus number of pulses for varistor 50.

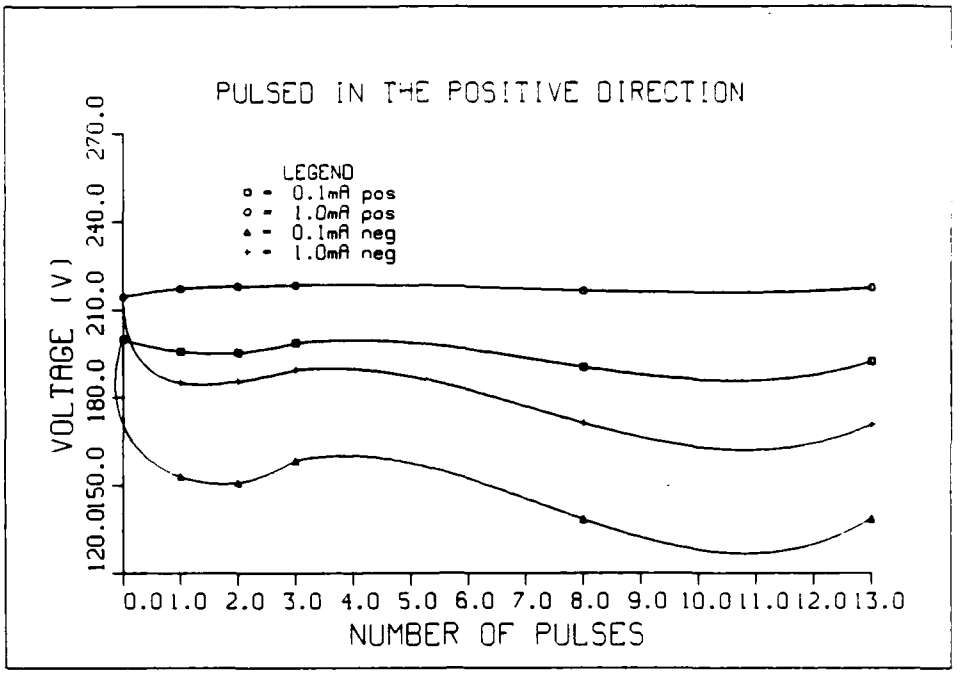

Figure B-21. Clamping voltage versus number of pulses for varistor 51.

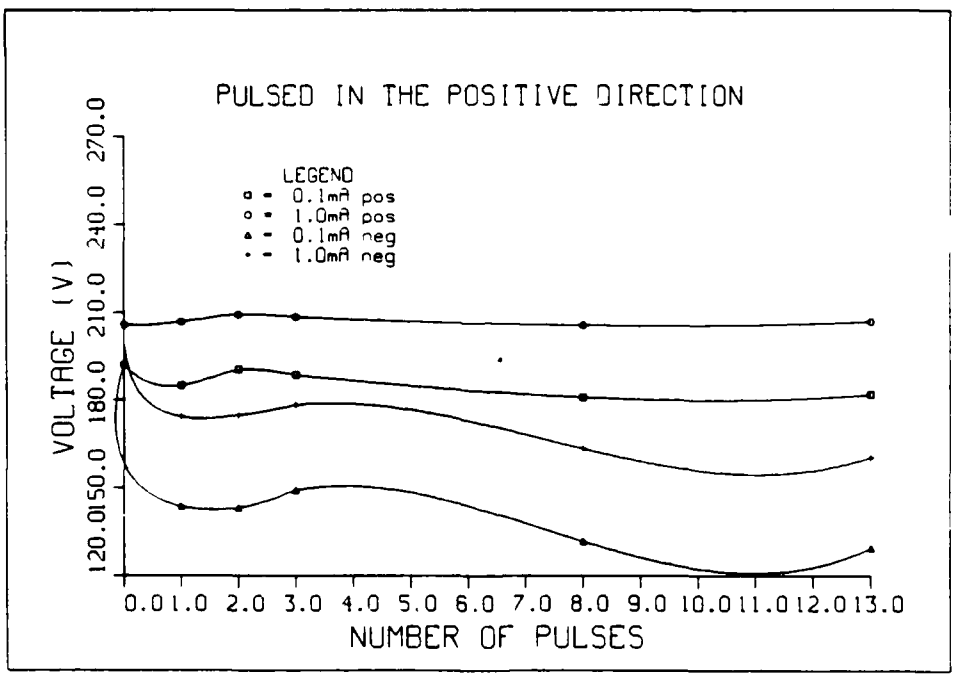

Figure B-22. Clamping voltage versus number of pulses for varistor 52.

APPENDIX C

CLAMPING VOLTAGE DATA AND I-V CURVE DATA FOR VARISTOR 21

Appendix C contains the data for the plots in Appendix B and the I-V curve data for varistor 21. These I-V curve data were used in the sample calculations in the report.

Table C-1. GE metal oxide varistor V33MA1A.

No.		Number of Cumulative Pulses 0	1	2	3
	Pulsed Positive				
1	0.1 mA pos	23.80	4.87	3.91	3.30
	1 mA pos	26.73	11.22	7.76	7.60
	0.1 mA neg	23.50	4.23	3.02	2.93
	1 mA neg	26.50	9.67	7.31	6.93
	Pulsed Positive				
2	0.1 mA pos	35.20	29.98	28.34	28.91
	1 mA pos	39.02	33.56	32.79	32.66
	0.1 mA neg	34.78	26.14	25.80	25.83
	1 mA neg	38.32	32.52	31.76	32.69
	Pulsed Negative				
3	0.1 mA pos	32.35	19.49	18.72	19.12
	1 mA pos	35.34	25.55	24.73	24.21
	0.1 mA neg	32.21	21.67	21.78	21.29
	1 mA neg	35.49	27.05	26.27	25.74
	Pulsed Negative				
4	0.1 mA pos	34.29	7.42	7.94	7.54
	1 mA pos	38.63	15.74	15.28	14.69
	0.1 mA neg	32.31	10.04	9.67	9.07
	1 mA neg	37.68	18.72	17.97	16.91
	Pulsed Alternating				
5	0.1 mA pos	34.73	19.14	18.97	20.55
	1 mA pos	37.95	27.51	26.62	26.88
	0.1 mA neg	34.81	24.53	23.81	19.97
	1 mA neg	38.01	30.15	29.23	26.42

Table C-2. GE metal oxide varistor V47AZ7.

No.		Number of Cumulative Pulses 0	1	2	3
	Pulsed Positive				
21	0.1 mA pos	43.45	36.00	38.65	38.67
	1 mA pos	47.43	44.90	45.98	45.86
	0.1 mA neg	43.26	25.41	28.85	31.27
	1 mA neg	47.68	38.09	40.15	41.41
	Pulsed Positive				
22	0.1 mA pos	44.92	44.50	45.12	42.49
	1 mA pos	48.89	49.92	50.41	47.55
	0.1 mA neg	45.35	36.60	36.86	38.05
	1 mA neg	49.02	45.92	46.39	45.93
	Pulsed Negative				
23	0.1 mA pos	41.91	32.47	33.64	35.14
	1 mA pos	45.53	42.34	42.78	43.23
	0.1 mA neg	42.29	40.72	41.58	41.57
	1 mA neg	45.68	45.84	46.11	46.03
	Pulsed Negative				
24	0.1 mA pos	42.14	30.20	31.56	32.27
	1 mA pos	45.68	41.61	42.09	42.10
	0.1 mA neg	42.39	38.94	39.29	39.18
	1 mA neg	46.07	45.80	45.92	46.01
	Pulsed Positive				
25	0.1 mA pos	44.51	29.70	36.35	36.35
	1 mA pos	48.44	41.98	43.57	43.45
	0.1 mA neg	46.07	20.13	29.51	29.18
	1 mA neg	49.56	33.60	38.70	38.99

Table C-3. GE metal oxide varistor V275LA40A.

No.		Number of Cumulative Pulses 0	1	2	3	8
	Pulsed Positive					
30	0.1 mA pos	338.58	339.81	340.27	339.80	
	1 mA pos	392.10	394.25	395.70	395.14	
	0.1 mA neg	338.55	319.80	325.14	324.21	
	1 mA neg	392.48	380.53	383.86	382.82	
	Pulsed Positive					
31	0.1 mA pos	444.33	427.22	425.72	428.30	423.00
	1 mA pos	468.60	470.80	474.12	475.50	474.33
	0.1 mA neg	445.92	381.09	376.80	376.78	369.69
	1 mA neg	470.14	443.11	440.66	436.22	427.75
	Pulsed Negative					
32	0.1 mA pos	387.15	389.84	371.44	369.74	359.54
	1 mA pos	432.35	437.20	430.65	428.20	418.85
	0.1 mA neg	386.71	364.10	383.40	384.24	384.45
	1 mA neg	432.85	423.67	437.80	439.40	440.70
	Pulsed Negative					
33	0.1 mA pos	381.22	359.81	359.71	359.60	424.08
	1 mA pos	421.05	410.80	410.67	409.39	374.50
	0.1 mA neg	380.52	379.77	381.33	383.01	479.88
	1 mA neg	420.17	424.58	426.66	427.61	436.66

Table C-4. GE metal oxide varistor V250PA40C.

No.		Number of Cumulative Pulses 0	1	2	3	8	13
	Pulsed Positive						
40	0.1 mA pos	383.01	379.70	360.35	355.66	315.75	329.71
	1 mA pos	402.57	403.37	403.26	399.99	385.65	389.77
	0.1 mA neg	385.33	361.44	344.44	338.92	299.42	304.74
	1 mA neg	403.75	400.74	390.82	388.34	363.48	362.40
	Pulsed Positive						
41	0.1 mA pos	369.71	369.75	369.62	368.70	363.66	366.83
	1 mA pos	397.77	397..67	399.24	399.71	398.56	400.02
	0.1 mA neg	370.06	351.06	342.44	341.94	329.76	326.81
	1 mA neg	369.94	392.45	386.31	385.11	377.63	374.31
	Pulsed Positive						
42	0.1 mA pos	358.90	329.76	313.06	304.24	290.33	326.81
	1 mA pos	381.75	374.34	369.65	366.76	359.78	353.52
	0.1 mA neg	359.81	314.69	296.36	290.41	278.40	271.31
	1 mA neg	382.43	363.18	357.55	354.22	343.77	337.85
	Pulsed Positive						
43	0.1 mA pos	386.42	376.83	376.05	377.50	374.56	375.66
	1 mA pos	406.20	402.03	405.36	404.33	404.51	405.88
	0.1 mA neg	387.38	357.85	343.50	348.28	337.97	334.75
	1 mA neg	406.87	395.31	386.46	384.79	384.14	382.00
	Pulsed Positive						
44	0.1 mA pos	350.43	341.16	341.33	342.13	338.68	339.90
	1 mA pos	373.46	371.46	371.92	372.80	372.72	373.62
	0.1 mA neg	351.42	314.70	312.80	313.10	300.56	295.29
	1 mA neg	374.20	357.35	357.83	356.71	349.22	345.36

Table C-5. GE metal oxide varistor V130HE150.

No.		Number of Cumulative Pulses 0	1	2	3	8	13
	Pulsed Positive						
50	0.1 mA pos	189.35	190.62	184.18	185.50	178.55	177.81
	1 mA pos	204.26	209.05	206.08	206.32	202.90	205.32
	0.1 mA neg	189.55	167.24	147.66	153.91	138.18	132.98
	1 mA neg	204.51	193.75	178.33	182.21	168.38	165.06
	Pulsed Positive						
51	0.1 mA pos	199.92	195.62	195.20	198.61	190.38	192.16
	1 mA pos	214.28	217.01	217.79	218.31	216.42	217.30
	0.1 mA neg	200.49	152.99	150.80	158.39	138.44	138.63
	1 mA neg	214.48	184.97	185.52	189.45	171.26	170.68
	Pulsed Positive						
52	0.1 mA pos	192.07	185.00	190.43	188.52	180.95	181.97
	1 mA pos	205.70	206.80	209.27	208.42	205.62	206.91
	0.1 mA neg	192.29	143.65	143.21	149.25	131.79	129.53
	1 mA neg	205.90	174.26	174.87	178.38	163.40	160.53

Table C-6. I-V curve and AC power.

Varistor Type: V47ZA7			Charging Voltage:
Varistor No.: 21			Cumulative No. of Pulses:
Date: 8/6/85 Time: 1:50			Cumulative Energy: 0

Positive Polarity Measurement

R (kΩ)	V_R (V)	I_v	V_v (V)
995.8	0.09958	100 nA	0.83
99.6	0.0996	1 uA	8.56
99.6	0.4980	5 uA	32.56
9.98	0.0998	10 uA	38.84
9.98	0.499	50 uA	42.25
1	0.1	0.1 mA	43.45
1	0.5	0.5 mA	46.07
0.1	0.1	1 mA	47.43
0.1	1	10 mA	51.87

AC power dissipation at $V_{m(AC)}$ (130 V) 0.9 mW
AC power dissipation at 1 mA 20 mW

Negative Polarity Measurement

R (kΩ)	V_R (V)	I_v	V_v (V)
995.8	0.9958	100 nA	0.86
99.6	0.0996	1 uA	8.50
99.6	0.4980	5 uA	32.41
9.98	0.0998	10 uA	38.12
9.98	0.499	50 uA	41.85
1	0.1	0.1 mA	43.26
1	0.5	0.5 mA	46.38
100	0.1	1 mA	47.68
100	1	10 mA	52.30

AC power dissipation at $V_{m(AC)}$ (130 V) 0.9 mW
AC power dissipation at 1 mA 19.8 mW

Table C-6. Continued.

Varistor Type: V47ZA7	Charging Voltage:
Varistor No.: 21	Cumulative No. of Pulses: 1+
Date: 8/9/85 Time: 12:53	Cumulative Energy:

Positive Polarity Measurement

R (kΩ)	V_R (V)	I_v	V_v (V)
995.8	0.09958	100 nA	0.60
99.6	0.0996	1 uA	4.61
99.6	0.4980	5 uA	13.96
9.98	0.0998	10 uA	18.81
9.98	0.499	50 uA	31.18
1	0.1	0.1 mA	36.00
1	0.5	0.5 mA	42.69
0.1	0.1	1 mA	44.90
0.1	1	10 mA	51.00

AC power dissipation at $V_{m(AC)}$ (130 V) 10.3 mW
AC power dissipation at 1 mA 18.6 mW

Negative Polarity Measurement

R (kΩ)	V_R (V)	I_v	V_v (V)
995.8	0.9958	100 nA	0.62
99.6	0.0996	1 uA	4.10
99.6	0.4980	5 uA	10.38
9.98	0.0998	10 uA	13.91
9.98	0.499	50 uA	21.98
1	0.1	0.1 mA	25.41
1	0.5	0.5 mA	34.12
100	0.1	1 mA	38.09
100	1	10 mA	48.07

AC power dissipation at $V_{m(AC)}$ (130 V) 9.7 mW
AC power dissipation at 1 mA 18.7 mW

Table C-6. Continued.

Varistor Type: V47ZA7 Charging Voltage:
Varistor No.: 21 Cumulative No. of Pulses: 2
Date: 8/13/85 Time: 10:00 Cumulative Energy:

Positive Polarity Measurement

R (kΩ)	V_R (V)	I_v	V_v (V)
995.8	0.09958	100 nA	0.70
99.6	0.0996	1 uA	5.90
99.6	0.4980	5 uA	18.03
9.98	0.0998	10 uA	23.30
9.98	0.499	50 uA	34.90
1	0.1	0.1 mA	38.65
1	0.5	0.5 mA	43.78
0.1	0.1	1 mA	45.98
0.1	1	10 mA	51.45

AC power dissipation at $V_{m(AC)}$ (130 V) 5.9 mW
AC power dissipation at 1 mA 18.6 mW

Negative Polarity Measurement

R (kΩ)	V_R (V)	I_v	V_v (V)
995.8	0.9958	100 nA	0.77
99.6	0.0996	1 uA	5.50
99.6	0.4980	5 uA	12.82
9.98	0.0998	10 uA	16.60
9.98	0.499	50 uA	25.04
1	0.1	0.1 mA	28.85
1	0.5	0.5 mA	37.12
100	0.1	1 mA	40.15
100	1	10 mA	49.12

AC power dissipation at $V_{m(AC)}$ (130 V) 5.6 mW
AC power dissipation at 1 mA 19.3 mW

Table C-6. Concluded.

Varistor Type: V47ZA7	Charging Voltage:
Varistor No.: 21	Cumulative No. of Pulses: 3
Date: 8/14/85 Time: 12:59	Cumulative Energy:

Positive Polarity Measurement

R (kΩ)	V_R (V)	I_v	V_v (V)
995.8	0.09958	100 nA	0.82
99.6	0.0996	1 uA	7.09
99.6	0.4980	5 uA	20.64
9.98	0.0998	10 uA	26.27
9.98	0.499	50 uA	35.58
1	0.1	0.1 mA	38.67
1	0.5	0.5 mA	43.95
0.1	0.1	1 mA	45.86
0.1	1	10 mA	51.50

AC power dissipation at $V_{m(AC)}$ (130 V) 6.2 mW
AC power dissipation at 1 mA 18.7 mW

Negative Polarity Measurement

R (kΩ)	V_R (V)	I_v	V_v (V)
995.8	0.9958	100 nA	0.88
99.6	0.0996	1 uA	6.43
99.6	0.4980	5 uA	15.90
9.98	0.0998	10 uA	19.76
9.98	0.499	50 uA	28.08
1	0.1	0.1 mA	31.27
1	0.5	0.5 mA	38.61
100	0.1	1 mA	41.41
100	1	10 mA	49.56

AC power dissipation at $V_{m(AC)}$ (130 V) 5.5 mW
AC power dissipation at 1 mA 18.9 mW

END

10-86

DTIC